Lasers in Manufacturing and Materials Processing (2023) 10:77–117
https://doi.org/10.1007/s40516-022-00200-7

A Systematic Literature Review on Laser Welding of NiTi SMA

Soumya Ranjan Parimanik[1] · Trupti Ranjan Mahapatra[1] · Debadutta Mishra[1]

Accepted: 30 November 2022 / Published online: 13 December 2022
© The Author(s), under exclusive licence to Springer Science+Business Media, LLC, part of Springer Nature 2022

Abstract

In this paper, a systematic literature review (SLR) approach has been implemented to show up the research progress on the joining of Nitinol (NiTi) Shape Memory Alloy (SMA) using laser. The properties of NiTi alloy, like the shape memory effect (SME), super-elasticity and biocompatibility, endure it as a desirable material in several high-performance applications. Owing to the extensive use of NiTi SMAs in medical devices, micro-electrical components, aerospace industries etc. joining of this alloy has been a subject of investigation and attracted the attention of the scientific community. Considering its unique characteristics, getting a proper joining of NiTi alloys with self as well as other materials is not only tough but also challenging. Therefore, literature on the advancements in the joining of NiTi alloys is reviewed systematically. Various challenges and ranges of the scope of research during similar and dissimilar joining are addressed and summarized. The weld joint characteristics such as the tensile strength, microhardness, corrosion resistance and microstructural properties are also outlined. Different optimization techniques implemented to obtain the optimum parameter setting during welding and/or machining of these distinctive materials are appraised. The research gaps referred to the domain are identified and deliberated.

Keywords Systematic literature review (SLR) · NiTi alloy · SMA · Joining · Welding · Optimization

✉ Trupti Ranjan Mahapatra
trmahapatra_pe@vssut.ac.in

[1] Department of Production Engineering, Veer Surendra University of Technology, Odisha 768018, India

Introduction

Titanium nickelide, also called Nitinol (NiTi), is an equiatomic alloy of Ni and Ti. NiTinol comes under the smart materials category. It can memorize its original shape and when mechanical load or heat is applied, it returns to its original shape [1, 2]. This material comes under a group of shape memory alloys (SMA). It has properties like shape memory, pseudo-elasticity, biocompatibility, etc. [3, 4]. The SMAs have lately been used in the field of micro-electromechanical systems (MEMS) due to their high performance, excellent resistance to fatigue and corrosion [5, 6]. SMAs are capable of returning to their original shape from the deformed shape when heat or mechanical load is applied [1]. Another category of NiTi alloys exhibit superelastic properties [7] that allows them to undergo large deformation and regain the undeformed shape up on removal of the applied load. However, because of restrictions like the high rates of work hardening or rapid tool deterioration, the machining of NiTi alloys is quite challenging [8]. NiTinol is gaining more attraction in various manufacturing industries owing to its unique properties. So, joining them is becoming the centre of interest as well as more challenging. Laser welding is a cost-effective and reliable methodology for joining NiTi sheets, wires, and tubes [9]. A low thermal influence which prompts to have deep penetration and a smaller welding area is one of the advantages of this process [9, 10]. Shape Memory Effect (SME) and Super-elasticity impacts of the welded part can be altered because of the heat applied. This in turn strongly affects the microstructure and chemical composition of the material and subsequently changes the temperature of phase transformation of the welded area [11]. Amidst other methods, the laser welding process is favourably used for joining NiTi alloys of different shapes as wires or sheets. Laser is replacing the traditional processes for machining and joining operation like cutting, drilling, welding etc. [12]. The laser welding method is economic for high precision and high-performance applications in comparison to the other joining processes.

The present work attempts to execute the systematic literature review (SLR) methodology to recognize the challenges and opportunities related to the joining of NiTi SMAs in similar as well as dissimilar combinations. In addition to the solid-state and fusion methods, special emphasis is given to laser welding as this technique have been most studied and investigated in this domain. A special section is devoted to the numerous existing and improved optimization techniques utilized by the researchers in an attempt to optimise the process parameters while handling the NiTi SMAs.

SLR Methodology

The SLR can be described as the quantitative method of identifying, selecting, and analysing the scientific studies of the formulated problem. Comparative to the conventional literature review, SLR critically appraises research with less time consumption and more precision towards the research question [13]. The SLR helps the researcher to perform a scientific review systematically that is defining the problem

statement, selection of method, collection of data and analysis. Methodological analysis in SLR enables the researcher to identify the flaws in the work and provide better clarity to conclude the research problem. The SLR is originally used in medical practices, but it is gradually used by other sectors as well [14]. SLR has the following main activities [15].

- Identifying the proper scientific works via structured questions.
- Systematic screening of the research by assessing quality through meta-analysis.
- Analysis/interpretation of findings and understanding the research conclusion.

Because of these functions, SLR cannot be treated as a conventional review. In a traditional literature review, vast area is explored without following a systematic approach. However, SLR is focused on finding specific answers to the research questions providing the research strategy to the researchers for ease of understanding the process by which the progress is done. Moreover, the exclusion or inclusion criteria, given in SLR, is very much vital for the assessment of the article. For a literature review on the joining of NiTi, an exploratory search in Scopus and Web of Science (WoS) is carried out. A flow chart of the currently embraced methodology is depicted in Fig. 1. For the initial search related to the topic Boolean logic (AND, OR) is used. The combined search word used is ("Joining" OR "Welding") AND "NiTi" AND "Laser". These search words are used to get a wide range of literature for review pertaining to our study. For the selection of the papers obtained from the search, Preferred Reporting Items for Systematic Reviews and Meta-Analyses (PRISMA) [13, 14] is used. PRISMA is an evidence-based analysis that ensures a systematic review of papers. PRISMA method is primarily invented to assess the benefits of medical inventions. Later it is used in other platforms due to its effective analysis [15]. The search result from the Scopus is detailed under different sub-categories (shown in Fig. 2) as published papers over time, country/region, document type and subject area.

From the search in the Scopus and WoS database using the proposed SLR illustrated in Fig. 1, total of one hundred ninety-six (196) and one hundred forty four (144) results are obtained in the introduction phase, respectively. To minimize the broad area to a more specific research area, inclusion criteria of the articles are used. The criteria used are as follows: the keywords used are only available in title and abstract, published year is limited from 2010 to 2022, the paper should have been published in the form of a peer reviewed English research article excluding editorial letters and conference proceedings, only engineering is used as a subject area and the search of paper is limited to only English language. After limiting the search, one hundred twelve (112) articles from Scopus and one hundred twenty-eight (128) articles from WoS met the inclusion criteria. In next phase, content analysis of those papers is performed. In content analysis, ninety-two (92) numbers of papers are excluded, as they are common to both the database search. Further, the remaining papers are filtered to acquire articles only related to laser welding and sixty-nine (69) articles are excluded. Accordingly, a total of seventy-nine (79) papers are used for reviewing. During review of selected papers six articles are included by snowballing and citation chaining search and a total of eighty-five (85) numbers of papers are finalized for reviewing and interpretation purposes.

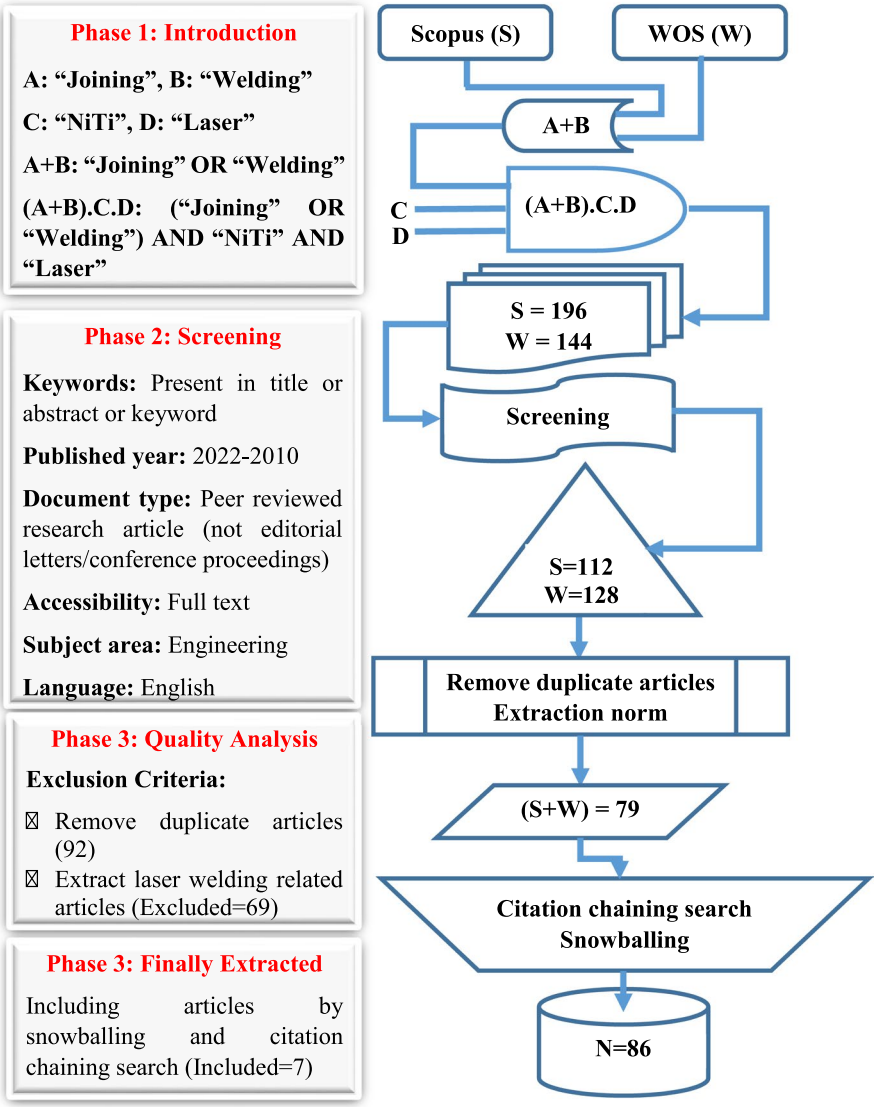

Fig. 1 Flow chart representing the present SLR

Appraisal of the Designated Literature

In order to perform detailed literature analysis and provide systematically the insights regarding the methods, evaluation criteria and evaluation procedure used in the proposed SLR, the literatures deliberated in the following sections are initially categorized by the type of application and characterization. With an increase in demand for more precise and intricate components, development

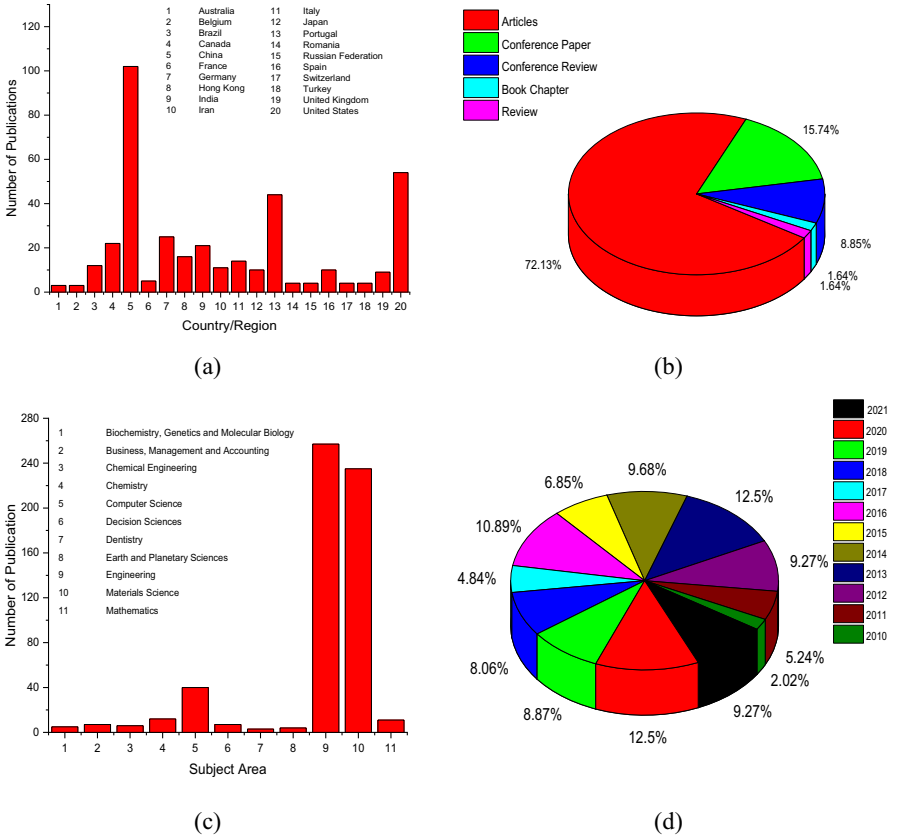

Fig. 2 Graphical presentation of searched result from Scopus database on published papers (**a**) Country/region-wise, (**b**) Type of paper/document, (**c**) Subject area and (**d**) Over time

in effective joining methods becomes necessary. Therefore, the development of effective joining of NiTi is immensely vital for the success of manufacturing the NiTi based alloy components. In this section, the analysis of scrutinised literature based on SLR methodology on joining of NiTi SMAs is carried out by dividing it into two important subsections as similar joining (NiTi-NiTi) and dissimilar joining (NiTi-other material). To achieve more clarity, the additional materials are further fractionated as ferrous and non-ferrous materials for the analysis of dissimilar joining. We note that, various fusion-based welding (Tungsten inert gas (TIG) welding, (Micro) Resistance welding) processes are suitably used for similar welding of NiTi sheets and wires. Likewise, diverse solid-state (Explosive welding, Friction-stir-welding (FSW), Ultrasonic welding [16], Adhesives joining, Brazing and soldering, Diffusion and reactive diffusion bonding) processes are congruously utilised for welding NiTi with other materials. However, the laser is the most admired welding technique for NiTi SMAs by virtue of its inherent characteristics (monochromaticity, high energy density, low heat input and

narrow Heat Affected Zone (HAZ)) [17]. The various aspects reported related to the laser welding of NiTi SMAs are summarized in Fig. 3 [5].

Similar Joining of NiTi Alloys

Various welding processes can cause localized changes in the welded area and yield properties of both base metal (BM) and welded zone (WZ). Early research [17, 18] on laser welding of NiTi wires with NiTi wires showed that after laser welding operation, the modifications in the materials for the welded part is not massive. Mostly, the welding of NiTi SMAs can be categorized as fusion welding process, solid-state welding process and brazing and soldering. The TIG welding is one of the basic conventional welding methods practised in many sectors. Ikai et al. [19] studied the effect of TIG welding on joining the NiTi wires (Ti-55.3 wt.% Ni SMA wire with outer diameter of 0.75 mm) and plates/sheets (Ti-55.1 wt.% Ni SMA sheet with a thickness of 0.2 mm and width of 8 mm). The SME is studied by testing the neighbourhood area of the weld with the help of heating–cooling and cyclic loading–unloading. A study of TIG welding on a near-equiatomic NiTi plate of 1.5 mm thickness is conducted by Oliveria et al. [20]. After welding, microstructure in the different zone is observed by an Optical microscope. At the HAZ, grain growth (Fig. 4a) and at fusion zone (FZ) fine equiaxed dendrite structure (Fig. 4b) is observed. During their experiment, they found that the SMA TIG weld part is showing full recovery of SME after 600 mechanical cycles. This typical characteristic accounts for the significant application of NiTi SMAs not only in commercial

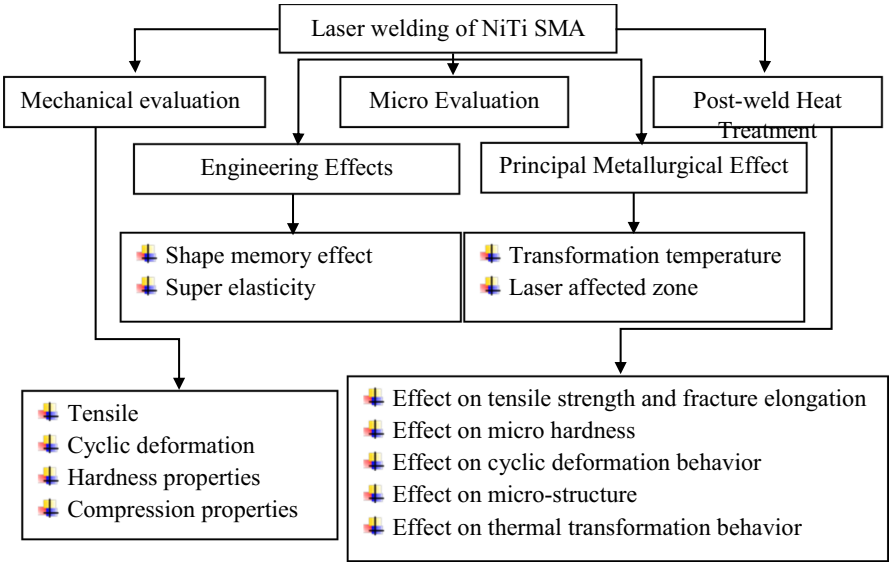

Fig. 3 Various aspects reported after Laser Welding of NiTi SMAs [5]

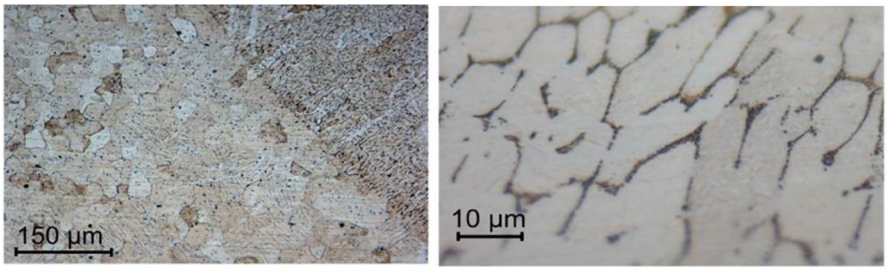

Fig. 4 Post welding micro-structure at (**a**) transition zone of HAZ and (**b**) FZ [20]

markets but also in delicate biomedical [21] and high-performance engineering industries.

These sectors also demand high dimensional accuracy that is non-viable through conventional joining processes. Therefore, various non-traditional joining processes are followed to meet the required dimensions. As already mentioned, laser welding is such a non-traditional joining process that is the most explored and implemented method, so far as joining of NiTi SMAs are concerned. This is because it has very low heat input and reduced extension of the FZ and HAZ [22]. Specifically, the Nd: YAG source is appropriate for joining of devices with intricate shapes because the heat input is low and accurate, energy density is low, HAZ and FZ are small, weld distortion and residual stress are low and welding speed is high [23]. Laser welding is a non-contact process in which the joining of materials takes place using a strong, monochromatic, coherent and highly directional laser beam [24]. Researchers have adopted Nd:YAG, pulsed [25], femtosecond type laser welding techniques to weld the NiTi alloy. However, laser welding of NiTi is difficult as functional properties (SE and SME) are affected due to thermal effects and post welding variation in chemical composition.

Laser welding of NiTi wires having a diameter of 100 µm is presented by Gugel et al. [26]. They have used Nd: YAG laser to weld the wires and studied the microstructure and different mechanical properties of the welded part. They observed changes in microstructure in the HAZ and FZ. The ultimate strength of the NiTi-NiTi wire joint is observed to be 75% more than the pure NiTi ultimate strength in the tensile strength test. As reported by Yao et.al. [17], similar laser welding is performed on NiTi wires and its effect on microstructure and SME are studied. It has been found that there is only a slight loss in the SME (< 5%). Datta. et.al. [27] also studied the laser input parameters like laser power and scan speed and their effect on similar laser welding of NiTi sheets. It is revealed that the formation of intermetallic compounds is responsible for the reduction of tensile strength after welding. Effect of various parameters on change in microstructure (Fig. 5), microhardness values and corrosion resistance are studied. Dong et.al. [28] studied the laser welding of NiTi and outlined the microstructural analysis within various zones using **Transmission Electron Microscopy (TEM)** and corrosion analysis. It is worthy to mention that the microstructural analysis of welded joints by using TEM is scarce. The

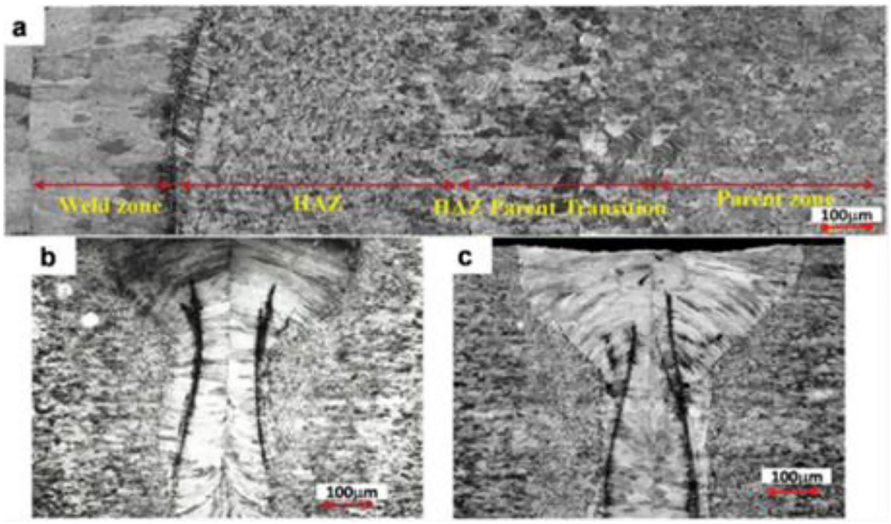

Fig. 5 (**a**) Effect of power on microstructural variation across weld bead with a constant scan speed of 5000 mm/min: (**b**) 800 W power and (**c**) 1000 W power [24]

results of the microstructural analysis revealed that laser welding affects the grain size of both FZ and HAZ [10] and the FZ has coarser grains than HAZ because of different temperatures at different zones with different solidification rates.

Chan and Man [29] studied the laser welding of similar NiTi wires and the post-weld heat treatment effect which resulted in superior mechanical and corrosion properties. Mirshekari et.al [23] also studied microscopy, mechanical properties and fracture morphologies of the similar NiTi laser weld using X-Ray diffraction analysis (XRD), energy dispersive spectroscopy (EDS), optical microscopy, scanning electron microscopy (SEM), tensile testing methods and Vickers microhardness tester. A decrease in microhardness values from the weld zone (WZ) towards the BM is observed whereas the tensile strength obtained from the WZ is on a higher side than the BM. A strain of 16% and tensile strength of 835 MPa is observed in their study. By selection of the optimal parameters for the welded joints, pores and micro-cracks can be avoided those appeared in the FZ [30]. It has been revealed that welding parameters like welding current and impulse width had more impact on the quality of the welded joint. Better welded joints are obtained when the welding current is set at 119A and impulse width at 2.5 ms. Oliveira et.al. [22] conducted an experimental study on the determination of residual stresses on laser-welded NiTi alloys by synchrotron radiation-based XRD. No distortions are found after butt laser welding of NiTi plates. However, the residual stresses within the welded joint are observed to be altered by applying proper post-weld heat treatment. Chan et.al. [31] investigated the effect of the welding parameters on the pseudo-elastic behaviour of fibre laser welding on NiTi foil using fractional

factorial (or Taguchi) design approach [1]. From the microstructural analysis, it has been found that the transformation temperature is highly related to Ni/Ti ratio and the morphology transition in the weld region is classified as a dendrite, planar and cellular (Fig. 6).

Dissimilar Joining of NiTi Alloys

Owing to the industrial demand there is a strong need for coherent joining of NiTi alloy with other (dissimilar) ferrous as well as non-ferrous materials. NiTi alloys have high demand in the medical sector, electronic device manufacturing, electro-mechanical based industries. Due to high cost of the NiTi alloys, it is not profitable to fabricate the entire components with the alloy. This leads to joining of the other suitable ferrous or non-ferrous metal or alloys with NiTi alloy to reduce the cost while upholding the functionality of the component. Various conventional materials such as stainless steel, $Ti6Al_4V$, MP35N, etc. are used for joining. However, joining of dissimilar material have its difficulties in terms of metallurgical and mechanical properties difference. In general, welding of dissimilar materials has many drawbacks like intermetallic compound formation in the weld pool, the difference in thermal properties, different properties of BMs etc. [31–34]. Therefore, researchers worked on several welding methods for the efficient joining of NiTi to other engineering materials [35–38]. The combination of NiTi alloy to stainless steel is desirable for many applications. But, when NiTi alloy is welded directly to stainless steel, brittle intermetallic compounds like $TiCr_2$ and $TiFe_2$ are formed. This contributes to brittle fracture and low tensile strength of the weld joint. This defect can be avoided by using a certain metallic interlayer between NiTi alloy and stainless steel. In transient liquid phase diffusion bonding, by using Ag–Cu interlayer, joint properties and weld microstructures can be improved. Zeng et al. [39] experimented on Ni wire and Cu sheets for dissimilar laser welding and studied the behaviour of functional fatigue. It is observed that, laser welding influenced the microstructure of the welded joint. The outcome of the research revealed that copper solution strengthened the

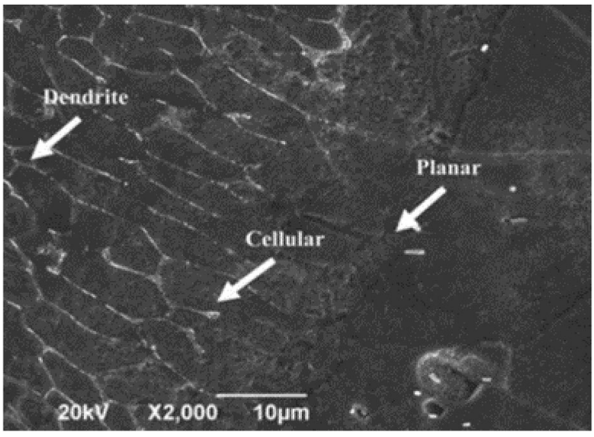

Fig. 6 Morphology transition in the NiTi weld [31]

weld. Huang et al. [40] studied the joining of NiTi to aluminium matrix composite by Friction stir processing (FSP). TIG has also opted for the welding of NiTi/Ti-Mo joints [41]. Fox et al. [42] studied the TIG butt welding of NiTi and 304 stainless steel (SS) tubes with the NiTi and 304SS tubes had 9.53 mm outer diameter and 5.72 mm and 6.22 mm inner diameter, respectively. After welding, the microstructure of the joint is observed and characterization is performed and no large-scale crack is observed at the joint (Fig. 7). Also, the weld can endure a shear strength larger than the yield strength of 304SS. This concludes that the welded part had sufficient Ni metal to prevent abrupt failure. Fukumoto et al. [43] performed friction welding of NiTi alloy and SS, both having a diameter of 2.5 mm and length of 30 mm. During welding, the formation of Fe_2Ti is observed, which is a brittle material resulting reduced joint strength after welding.

Use of Interlayer

In general, no filler material is required when joining NiTi to Ni–Ti, while in dissimilar ones, there is a need for interlayer to develop intermetallic compounds and to avoid atomic diffusion of the elements [22]. Yuhua et al. [44] conducted laser welding on the NiTiNb SMA with $Ti6Al_4V$ alloy. They found several types of cracks (longitudinal cracks, transverse liquid cracks, hot cracks, and crater cracks) on the dissimilar welded part. During observation they found that the number of crack is increasing as the laser power in increasing (Fig. 8). The same behaviour is also observed by other researchers as well [45]. Because of dissimilar welding, there is formation of different intermetallic compounds in the welded zone, namely $AlNbTi_2$, $NbNi_3$ and Ti_2Ni. The main reason of formation of crack is the brittleness of these intermetallic compounds. Because of these reasons an interlayer material is needed to reduce the brittle compound formation. Selection of proper interlayer or filler material helps in eliminating possible downsides due to dilapidation of the welding process [46]. Cobalt interlayer in laser welding of NiTi to $Ti6Al_4V$ can influence the chemical composition in the FZ, that leads to reduction in brittle Ti_2Ni formation [47]. In friction welding, Ni interlayer and laser brazing, the silver-based filler can be used to improve joint quality [48]. Pouquet et al. [49] utilized economically accessible AISI316L of thickness 0.47 mm and NiTi foils of thickness 0.34 mm with a pulsed Nd/YAG laser during dissimilar lap welded joint and observed an extensive

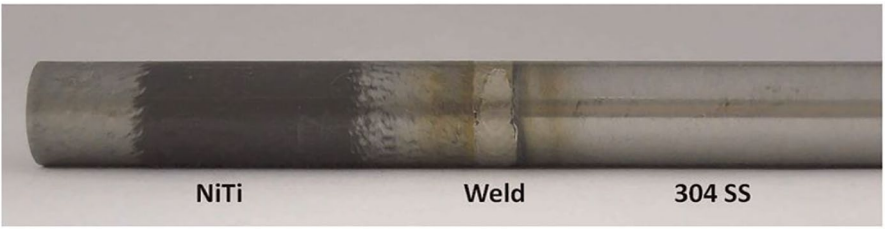

Fig. 7 Joint of NiTi and SS after TIG welding [42]

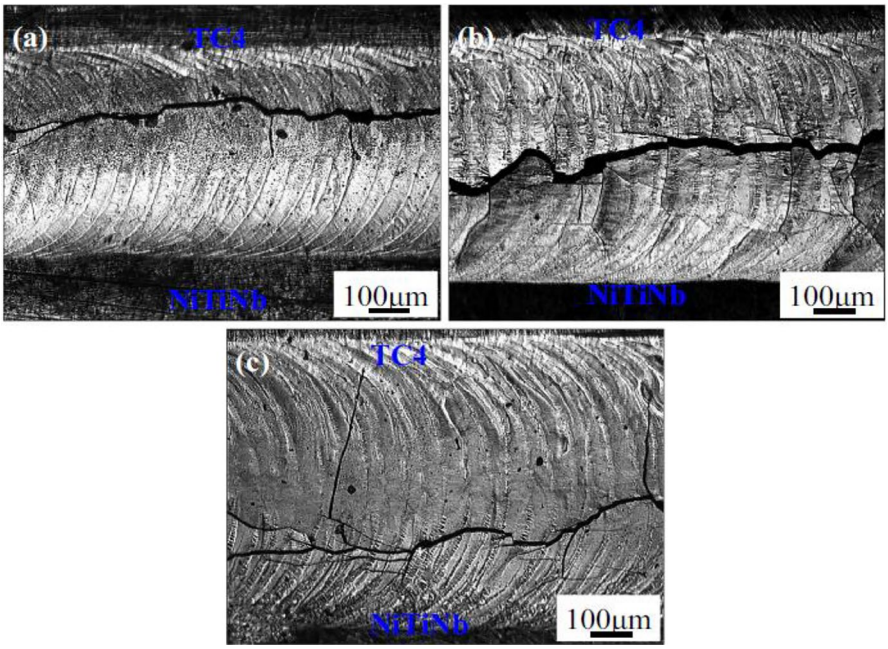

Fig. 8 Crack propagation with increasing laser power (W) of (**a**) 7.2; (**b**) 9.6; (**c**) 12 [44]

cracking as shown in Fig. 9a. However, by increasing the pulse duration or interaction time, uniform weld pool can be attained (Fig. 9b).

Li et al. [48] studied the laser welding of NiTi SMAs with stainless steel using a Ni interlayer between them (Fig. 10). After welding, they observed a dissimilar metal weld pool. The pool consists of BMs, WZ and HAZ. Swirling characteristics

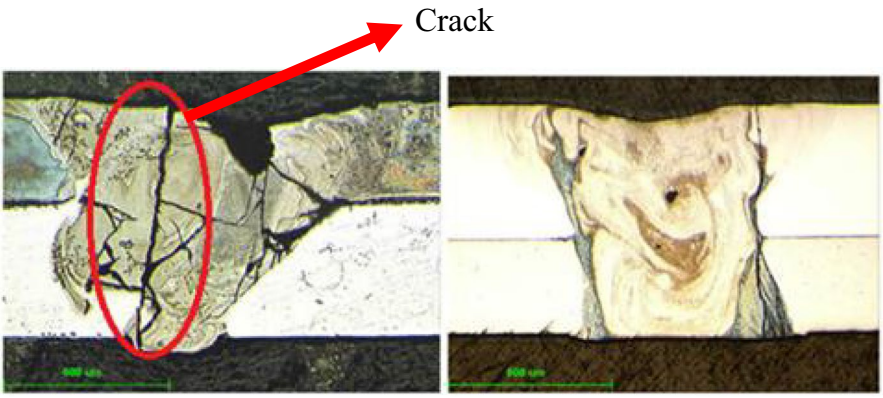

Fig. 9 NiTi and stainless-steel welding with stainless-steel interlayer (**a**) Formation of crack. (**b**) Uniform weld pool [49]

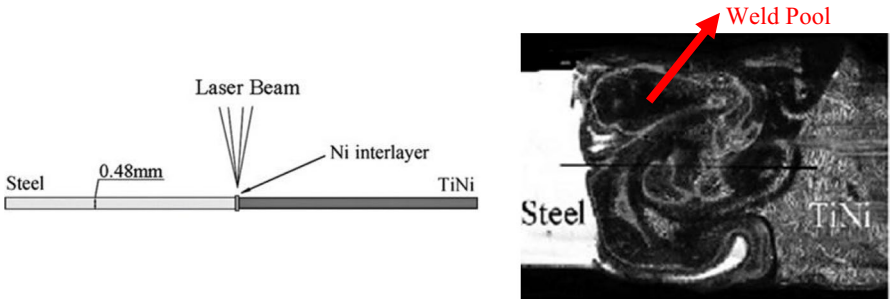

Fig. 10 (**a**) NiTi and stainless-steel welding with Ni interlayer (**b**) Macrostructure of Weld pool generated [48]

of weld pool are noticed because of the progression of liquid metal in weld pool (Fig. 10b).

Figure 11 shows weld Fe, Ni, Cr and Ti contents as a function of Ni interlayer thickness. When the Ni interlayer used is thick, the percentage of Ni is richer and the percentage of Cr, Ti and Fe will be lower in the WZ. Li et al. [48] observed that with increasing Ni interlayer thickness (100 µm from 10 µm), the Ni content in the weld increased to 66.41wt.% from 27.84wt.%. Also, a decrease in Cr (12.12wt.% to 5.29wt.%), Fe (40.43wt.% to 19.65wt.%) and Ti (19.61wt.% to 8.65wt.%) contents are observed in the weld. It indicates that the addition of more Ni interlayers decreases the chance of the formation of brittle intermetallic compounds. Oliveira et al. [50] studied the effect of Niobium interlayer in laser welding of NiTi- Ti6Al4V. Figure 12 shows the SEM microstructure in the weld interfaces and the weld centreline of the dissimilar welding of NiTi and stainless steel. It is noticed that across the FZ, the solidification mode changes from planar to cellular and then from cellular

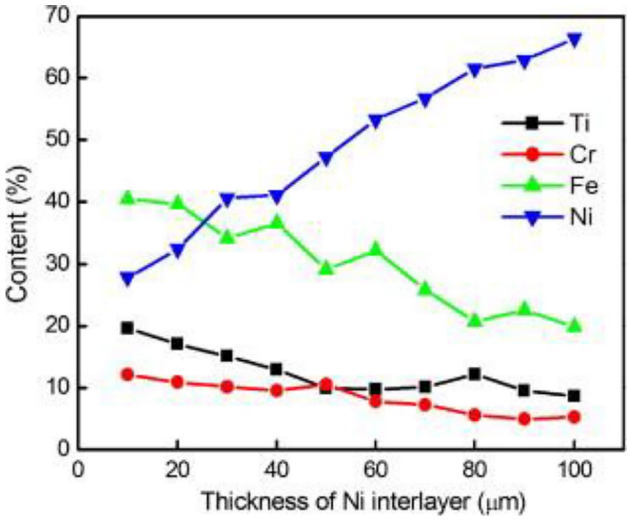

Fig. 11 Effects of thickness of Ni interlayer on % content of Cr, Fe, Ni and Ti in weld [48]

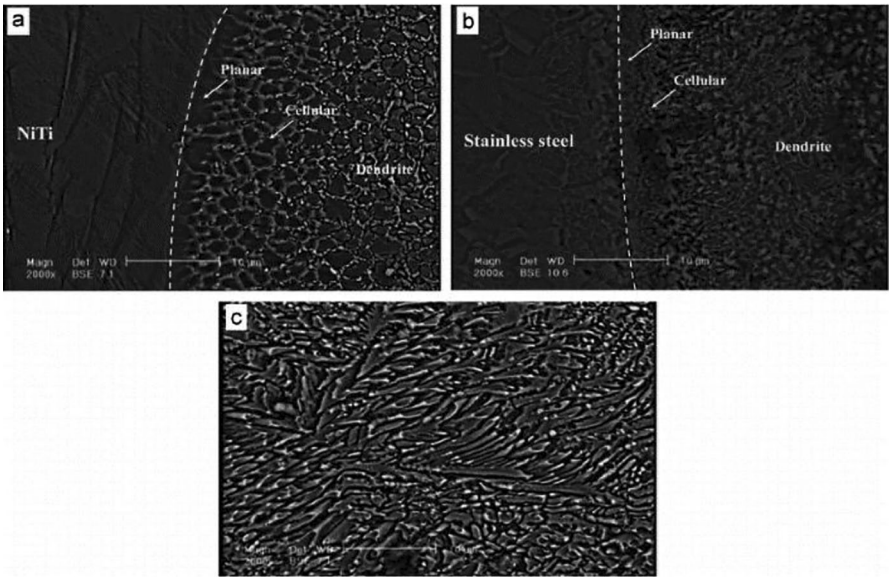

Fig. 12 SEM image of (**a**) weld interface boundary of NiTi, (**b**) weld interface boundary of SS and (**c**) weld centre line [23]

to dendrite. This behaviour is attributed to the increase in cooling rate from the WZ interface towards the weld centreline in both NiTi and stainless steel sides [23].

It is recommended that the formation of brittle intermetallic compounds can be reduced by using high enthalpy alloys (HEA). Wang et al. [51] studied the effect of HEA (CoCrFeNiMn) after laser welding of NiTi SMA and 304SS. They observed that the HEA has a diminishing influence on the formation of IMC by relieving the thermal stress of the welded part, which leads to a well-developed welded region. They also observed the formation of ductile (Fe, Ni) compound while using HEA as interlayer material.

Mechanical and Metallurgical Properties Evaluation

In this section, the recitation of technological characteristics as the tensile strength, microhardness, corrosion properties as well as microstructural characteristics after laser welding of NiTi alloys have been reviewed.

Tensile Strength

The measurement of tensile strength of the material after joining operation is vital owing to different intermetallic compound formation during welding. The formed compound may increase or decrease the tensile strength of the welded part according to the extent of their presence. Datta et al. [27] compared the tensile properties of NiTinol sheets before and after welding (Fig. 13). Decrease in tensile strength of

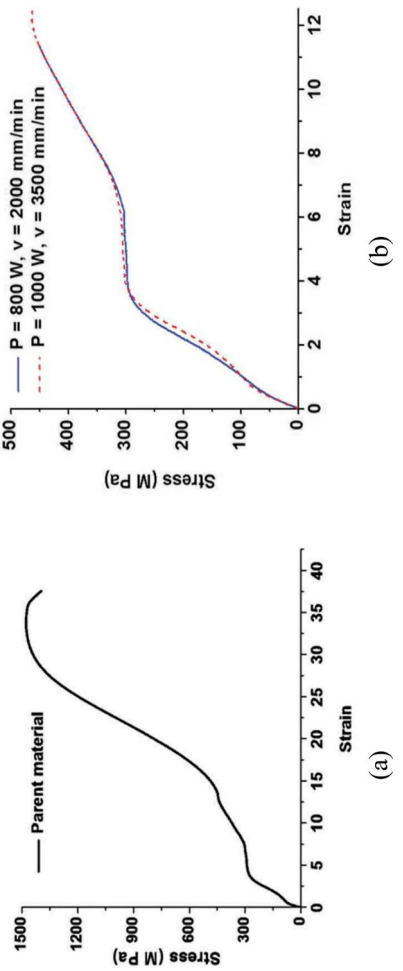

Fig. 13 Comparison of tensile strength result of (**a**) BM and (**b**) welded part at different combination of input parameter [27]

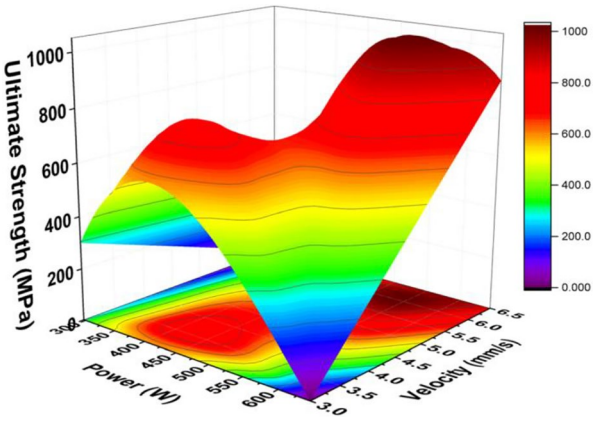

Fig. 14 3D plot of ultimate tensile strength of welded material [52]

the welded part in comparison to the parent material is observed from the figure. The change is strength is attributed to the increase in brittleness of the material during welding process because of increase in fine dendrite structure in the weld pool.

During tensile test after welding of NiTi super elastic material with NiTi SMA, Mehrpouya et al. [52] observed failure at the super elastic side of the joint. The maximum ultimate strength obtained for the weld is 1000 MPa as shown in Fig. 14. In friction welding of TiNi alloy with stainless steel (Fe_2Ti), which is a brittle material, intermetallic compound is produced. This compound decreases the joint strength of the weld. However, using Ni interlayer between the two materials, increase in the strength is noticed as the formation of Fe_2Ti is prevented [34, 53]. The variation in joint strength with rotational speed can be clearly noticed in Fig. 15.

Shamsolhodaei et al. [54] conducted a cyclic tensile experiment to test the superelasticity of the NiTi wire. The response of the test at room temperature and above (60℃) is shown in Fig. 16. In the case of low power (LP) weld, the residual strain changes from 0.4% to 1% for the 1st cycle and after ten cycles, respectively. Th residual strain is 1% and 1.9% after the 1st cycle and 10 cycles for high power (HP) laser

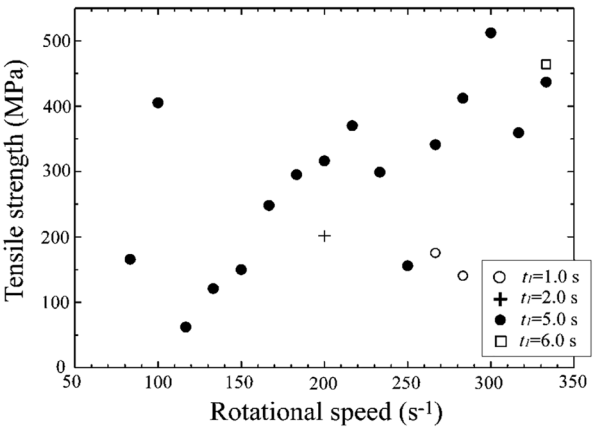

Fig. 15 Variation of tensile strength with rotational speed [43]

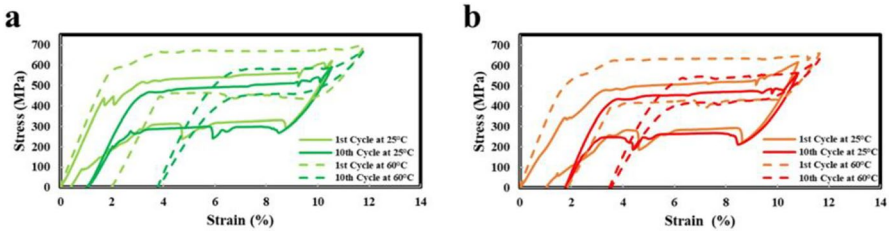

Fig. 16 Tensile cyclic response (**a**) HP weld sample and (**b**) LP weld sample [54]

weld. On the other hand, the strain values show a little to no difference when tested at 60℃. This results in the larger grains in FZ.

Ge et al. [55] studied the variation of shear force with the displacement (Fig. 17) with a constant welding speed of 3 mm/s. They observed with laser power, the strength of the joint increases initially but then decreases. This trend is attributed to the increase in heat supplied due to the gradual increase in power. Low laser power (900 W and 1000 W) does not have sufficient heat for a well welded joint causing low joining strength. On the other hand, high laser power (1200 W and 1300 W) may result in severe failure in welded surface. This also tends to decrease the strength of the joint after laser welding. The variation of tensile strength with respect to welding speed (Fig. 18) has also been studied. The variation of tensile strength follows the similar trend as that of the shear force (Fig. 18b). Low welding speed increases the heat input resulting excessive burning of the material and finally reducing the tensile strength. Similarly, high welding speed leads to shallow weld depth because of insufficient heat giving rise to reduced weld strength.

The tensile strength and stress–strain properties of welding samples along with the BM have been investigated in dissimilar combination (NiTi to 316L stainless steel) [56]. Results revealed that the use of interlayer increases the tensile strength nearly twice as compared to that of the cantered offset welding (Fig. 19a). However,

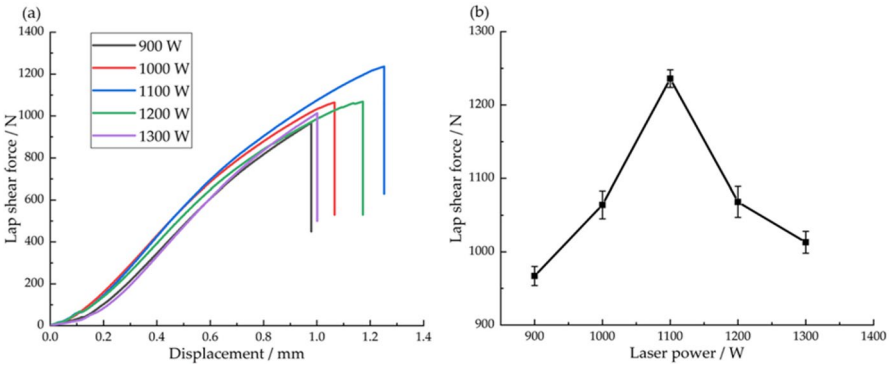

Fig. 17 (**a**) Shear force vs displacement plot; (**b**) variation of mean lap shear force with respect to various Laser power. [55]

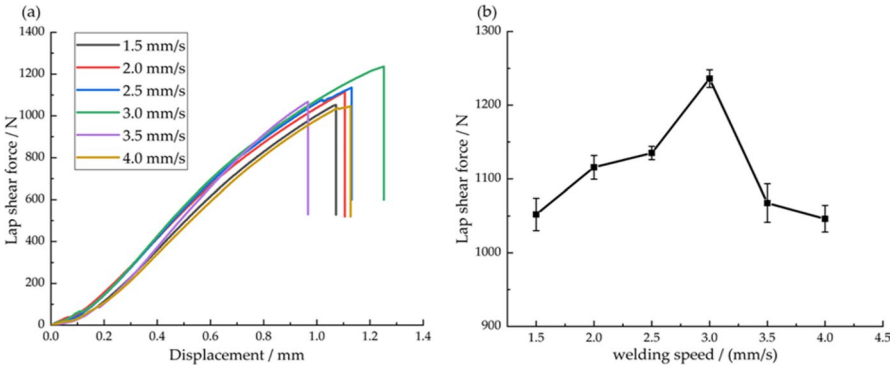

Fig. 18 (**a**) Tensile strength vs displacement plot; (**b**) variation of average lap tensile strength with respect to various welding speed. [55]

the offset laser welding is also showing nearly same tensile strength without the use of metallic interlayer. The offset laser welding method is reported to be preventing the formation of brittle intermetallic components and alters the microstructure of BM and WZ interface, which finally enhances the properties of the welded part. Figure 19c shows the zoomed view of the section "c" in marked in the Fig. 19b. The figure shows that the offsetting welding is not able to reach the required amount of stress value to show the martensite phase, it is failing just before reaching that stress level. None of the welded sample exhibit that level of stress to induce martensitic phase.

Figure 20 shows the stress–strain curves for the welded part along with the BM in dissimilar combination (NiTi and CuAlMn) [57]. The curve clearly indicates that

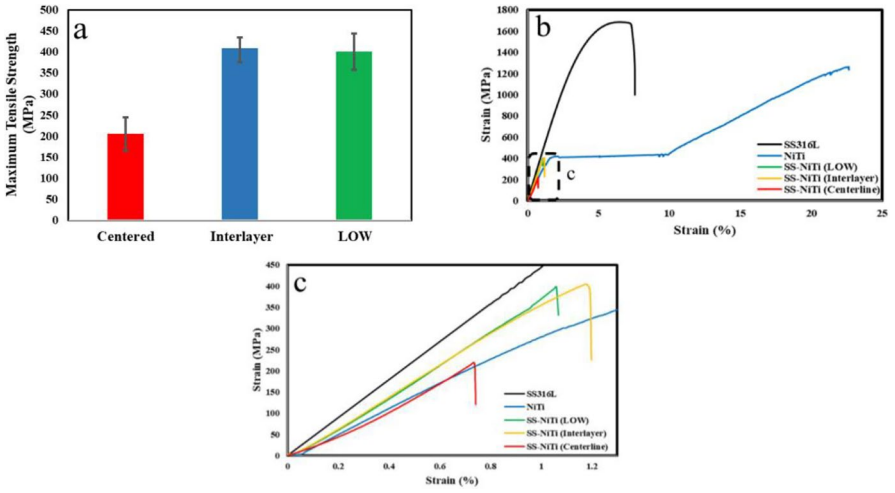

Fig. 19 (**a**) Tensile strength, (**b**) Stress vs strain curve and (**c**) zoomed view (of "c") [56]

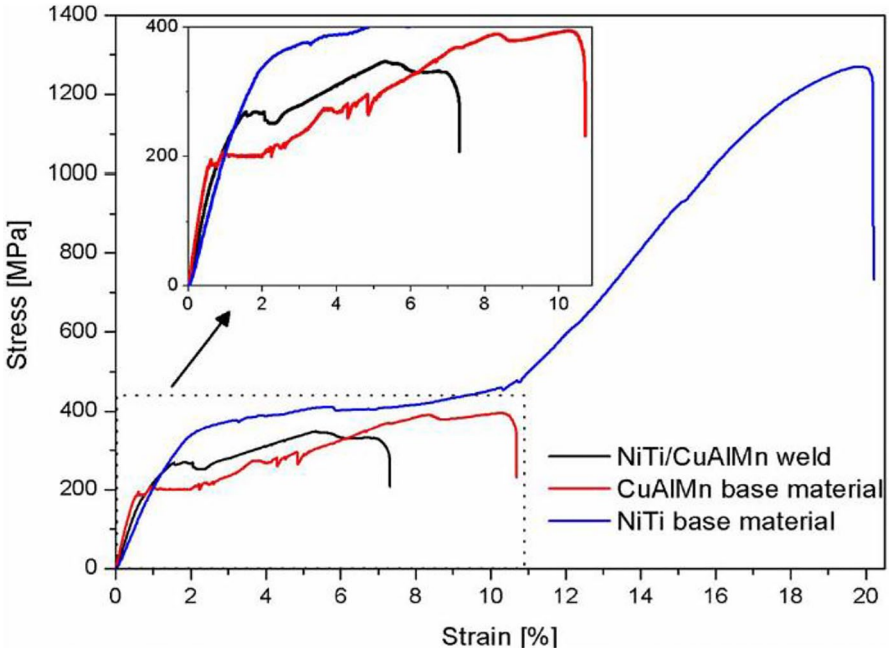

Fig. 20 Stress–strain curves of the NiTi and CuAlMn BM and their dissimilar joint [57]

the tensile strength as well as fracture strength of the NiTi BM is much higher than the other BM (CuAlMn) and the welded part. In addition to the fracture strength, the elastic state of the NiTi base material is also at a comparatively higher than the CuAlMn BM and the welded part. Additionally, Oliveira et al. [57] did not observe any HAZ in the side of CuAlMn because the superelastic properties of the material is enhanced prior to laser processing by heat treatment.

Microhardness

The hardness of the NiTinol differs in the BM zone, FZ and the HAZ during welding. This changes in hardness value are because of the different mechanical properties of the metal at various zones as well as the thermo-mechanical properties change during welding [58]. Datta et al. [27] investigated the changes in microhardness of the three zones of NiTi sheet after welding operation. Figure 21 shows the variation of microhardness along the centre line of the WZ to BM. They observed the gradual increasing hardness values from the weld pool zone to the BM. They attributed this variation along the centreline to the change in growth of the grain during solidification at different zones.

Mehrpouya et al. [58] observed a sharp decrease in hardness value when moving from BM to HAZ then after the values increases in the FZ (Fig. 22). They reported that the recrystallization, formation of some precipitates like (Ni_4Ti_3, Ni_3Ti, $NiTi_2$) and change in the grain structure are the main reason for the

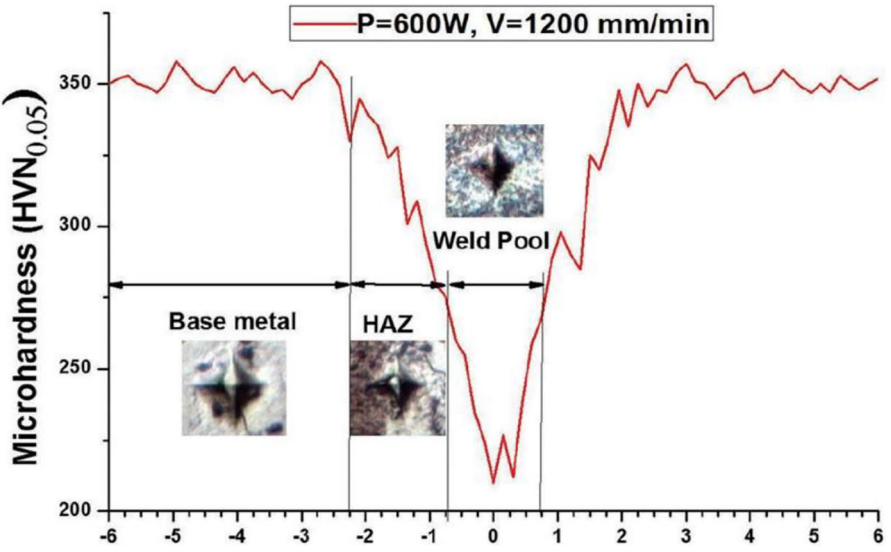

Fig. 21 Change of microhardness from the weld-bead to BM [27]

observed trend of change in microhardness values. Study on the dissimilar welding of NiTi super elastic and NiTi SMA wires by Mehrpouya et al. [52] (Fig. 23) showed that the super elastic side of the weld is harder than the shape memory side of the weld. Higher percentage of Ni in the super elastic side makes that side harder as compared to the SMA side. The Fig. 23 also shows that the hardness is gradually increasing from FZ towards the parent metal. Similar result is also observed when welding a NiTiCu wire with NiTi wire [59]. The NiTi side of the

Fig. 22 Vickers microhardness result of different zones of welding [58]

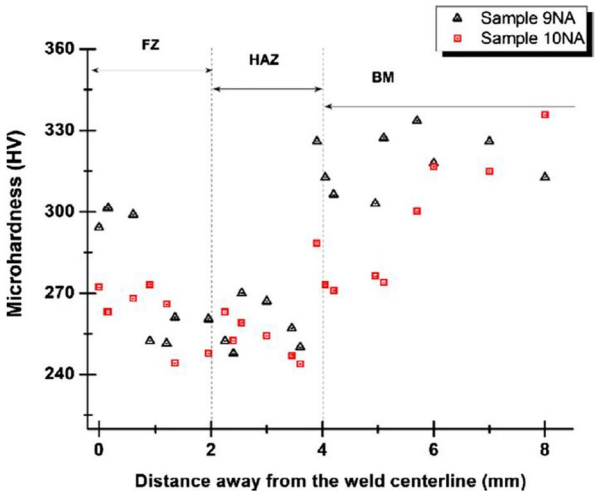

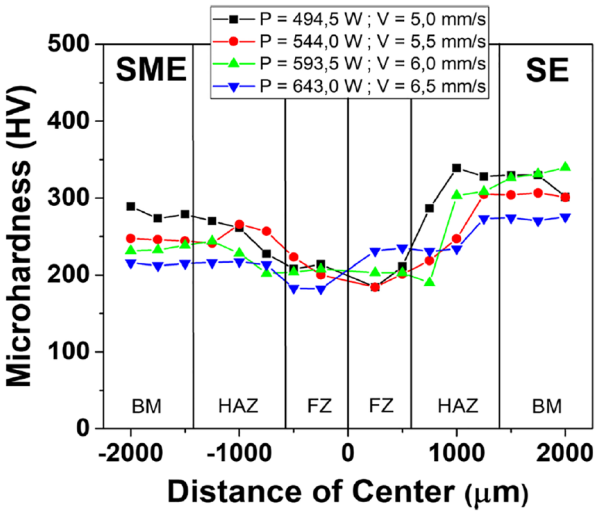

Fig. 23 Result of microhardness for laser welding of NiTi SME wire with NiTi SE wire [52]

joint is harder than NiTiCu side. This is since the NiTi is Ni rich as compared to NiTiCu wire.

Shamsolhodaei et al. [54] conducted a load-unload nanoindentation using a nanoindentation platform. The calculated residual depth and dissipated energy curves are shown in Fig. 24. For both residual depth and dissipated energy, the values are higher in FZ. Also, the said parameters is increasing gradually after unloading as observed from the curve. For both residual depth and dissipated energy, the values are higher in HP samples as compared to the LP samples within the FZ. This attributed to the presence of martensite phase in the HP sample. This lead to the conclusion that after the welding process, the superelasticity of the material degrades as a result of change of the critical yield strength to a lower value than the martensite transformation stress.

As observed from Fig. 25, a higher peak power tends to soften the NiTi wire but not the MP35N wire. This is the result of pre heat-treatment process of NiTi wires, which is not in the case of MP35N wire. It is apparent from the results that the hardness of the FZ is higher than the BM which is also reported by the other researchers [56–58, 61]. The hardness of the welded part in dissimilar welding can be reduced

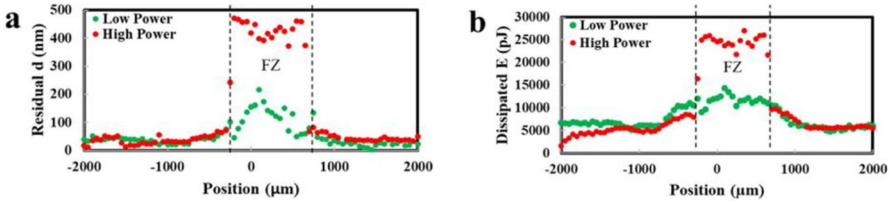

Fig. 24 Calculated load-unload nanoindentation parameter (**a**) residual depth and (**b**) dissipated energy [54]

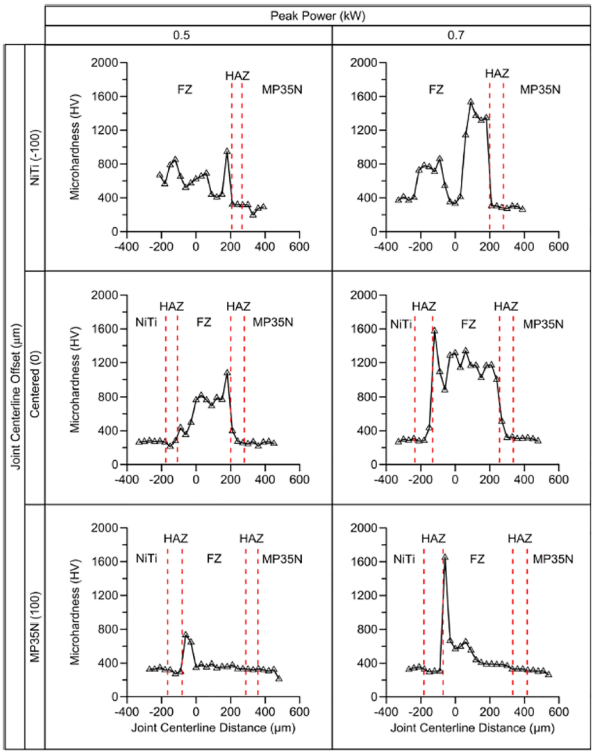

Fig. 25 Microhardness (HV) test values at different locations [60]

by the addition of Ni-powder during the welding. The same is explored by Asadi et al. [62] while joining NiTi alloy with AISI 304 SS. According to their results, the hardness of the welded zone is reduced by 43% when Ni powder is added.

Corrosion Property

In post weld corrosion test Datta et al. [27] found that the rate of corrosion in welded part is lower than that of the BM (Fig. 26). The corrosion test results for the welded part and the parent materials as reported by Costa et al. [41] is shown in Fig. 27. The tests are performed in Phosphate-buffered saline electrolytes. The results clearly show that the weld area is more corrosion resistant. This is owing to the decrease in nickel percentage in WZ with increase in Ti percentage to form a Ti–rich environment in the WZ. This leads to the formation of titanium oxide in the weld part which results in increasing corrosion resistance.

The corrosion properties of the laser pulsed, chemically etched (CE), laser processed and mechanically polished (LPMP) and laser processed and chemically etched (LPCE) NiTi strips are compared [63] using potentiodynamic cyclic polarization which is shown in Fig. 28. Laser pulsed and LPMP samples show a faster corrosion rate within the same current density region of 1.99×10^{-6} A/cm^2

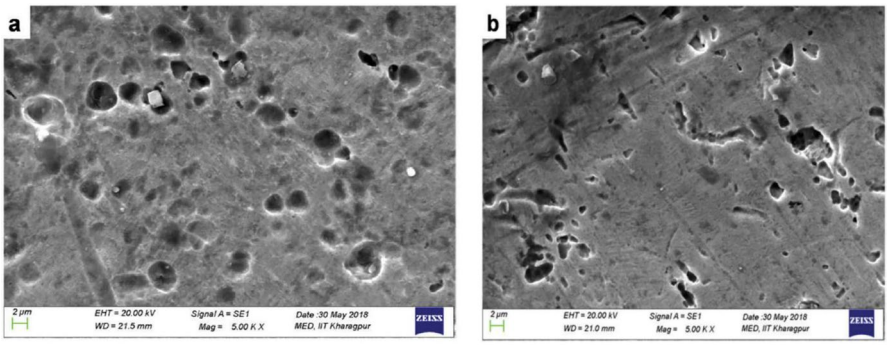

(a) (b)

Fig. 26 SEM micrograph of (**a**) parent material and (**b**) welded joint [27]

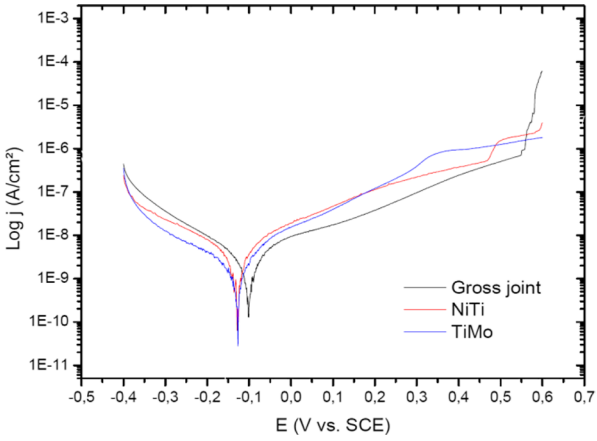

Fig. 27 Linear potentiodynamic polarization curves for gross joint, NiTi and TiMo [41]

to 4.56×10^{-6} A/cm^2. Lower values of breakdown potential and repassivation potential is also observed by Chan et al. [64]. They suggested that the observed low value of the potential is attributed to the materialization of surface oxidation during HP laser processing (Fig. 29). The presence of reactive materials at the surface decreases the corrosion potential values of LPMP (-461 mV) and LPCE (-319 mV) samples which implies the improvement in the corrosion resistance [63].

Differential Scanning Calorimetry (DSC)

It is well known that during the welding of NiTi alloy changes its transformation temperature significantly. The change in the temperatures during phase transformation of NiTi *i.e.*, austenite temperature and martensite temperature is measured by DSC test. The DSC is a material characterization test which describes the manner of physical properties change of a sample with temperature variation

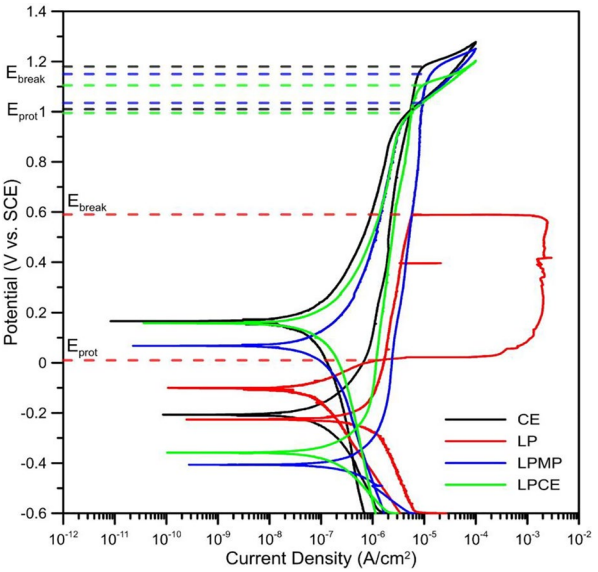

Fig. 28 Potentiodynamic cyclic curves [63]

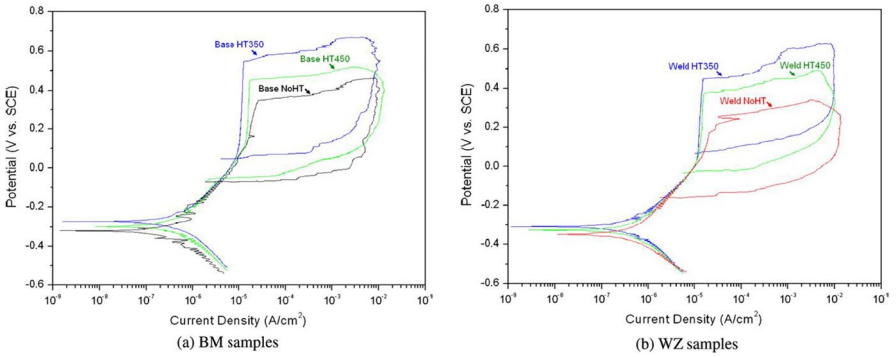

Fig. 29 Cyclic polarization Curve [64]

against time. Figure 30 shows the change in transformation temperatures of the BM and the WZ. This curve shows temperature of different phases of NiTi like austenite phase (B19/), martensite phase (B2) and rhombohedral phase (R) during heating and cooling. The change in phase from austenite to martensite is generally observed when heating the material and the reverse phase transformation is seen while cooling. The transformation temperatures of the welded metal are lower than the BM [40, 43]. This reduction in temperature after welding may be attributed to the presence of oxygen during welding [27]. The DSC test results for welding of NiTi sheet also shows the similar trend as that of the NiTi wires (Fig. 31).

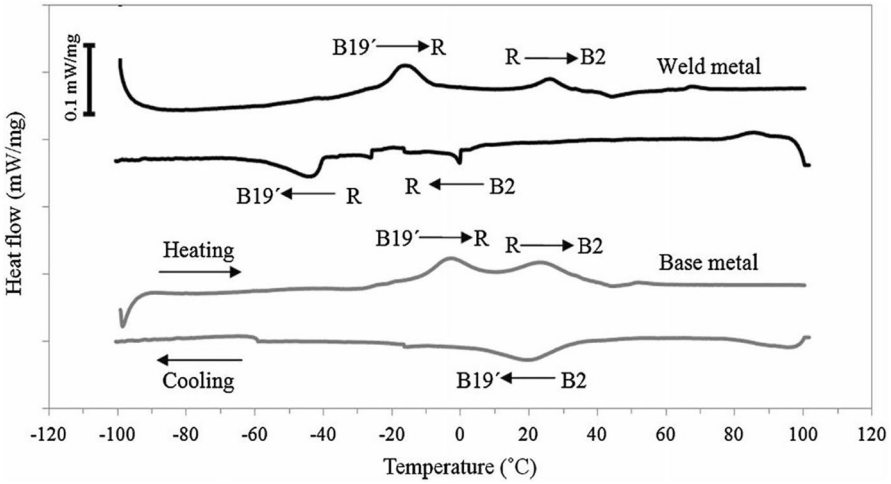

Fig. 30 DSC curve for WZ and BM of Ti-55 wt.% Ni wires [65]

Figure 32 shows the DSC results obtained by Pequegnat et al. [67] where the first set of peaks at comparatively lower temperatures for the LP zone of the sample than its adjacent zones. It can be clearly noticed from the Fig. 32b that the laser is welded very well as the depth of penetration is around 350 µm, which is relatively larger for laser processing.

Michael et al. [68] studied the change in DSC curve pattern with the help of mathematical model and compared them with two existing standard model, as shown in Fig. 33. The two types of mathematical model those are used for comparison are (Fig. 33e, f) and (Fig. 33c, d). It is observed that the peaks obtained for annealed wires (AW) are in skewed distribution with abrupted end part. The new proposed model provides lower error values than the two models. Between the two models, Fraser-Suzuki asymmetric Gaussian model provides nearly accurate result for skewed pattern whereas Cauchy model matches the top and bottom pattern of

Fig. 31 DSC curve of NiTi sheet metal [66]

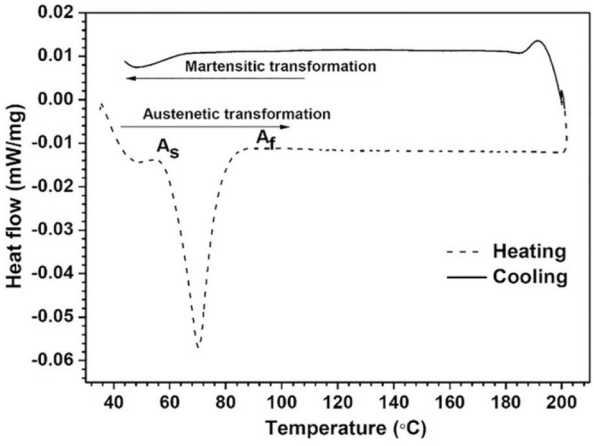

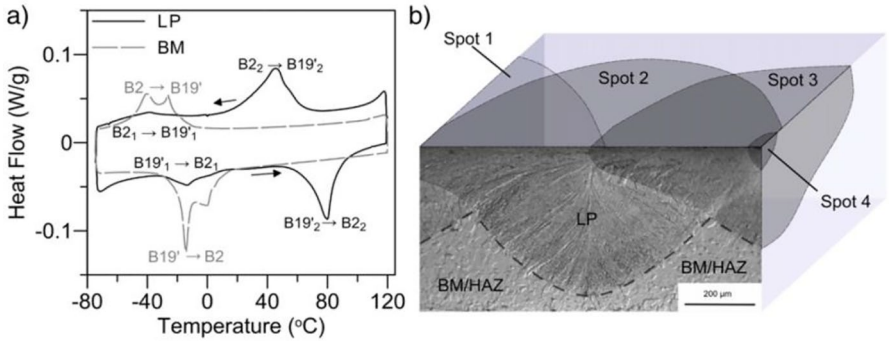

Fig. 32 (**a**) DSC curves for laser processed NiTi and BM, (**b**) locations of BM, LP and HAZ zone [67]

distribution. For processed wire (PW) samples, the peaks are more uniformly distributed. Unlike the AW samples, the Fraser-Suzuki asymmetric Gaussian model matches well with the PW DSC curves. They concluded that the proposed model works better to plot the fitted curves because it has more parameters those can be controlled better in comparison to the said standard models.

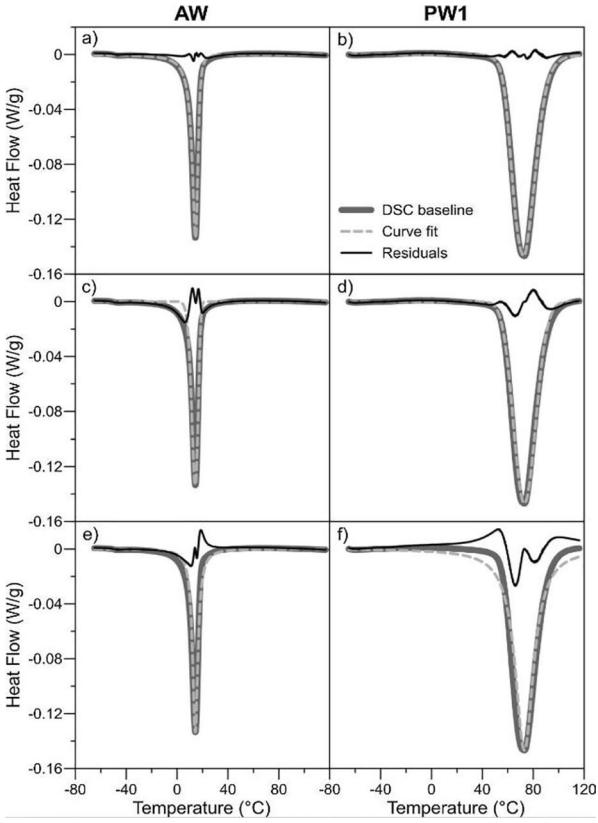

Fig. 33 Comparison plot for DSC of AW and PW samples [68]

In general, the yield strength and phase transformation temperatures of NiTi SMA are enhanced by cold working and followed by aging heat treatment. Panton et al. [60] did not find the R-phase transformation during the laser processing of annealed BM. They found Ti-intermetallic oxides at high transformation temperature. The formed oxides do not dissolve during the heat treatment process; therefore, they do not affect the transformation temperature. This shift in phase is shown in the Fig. 34. Another important factor which reduces the phase transformation temperature is the MP35N wire elements that work as Ms depressant. Because of the nature of welding (i.e., dissimilar type welding), there exist multiple phases (austenite and martensite) that are in contact with one another [60].

Microstructural Analysis

The SEM study on melted zone of the laser welded NiTi to NiTiCu by Mehrpouya et al. [69] showed that the grain boundary is divided into FZ and the HAZ. This separation of the two zones is shown in Fig. 35. Cross sectional view of NiTi-NiTiCu weld in Fig. 36 shows that the grains in the HAZ are finer than FZ grains. This trend in grain is because of the temperature difference between the two zones as well as the solidification process [58]. In FZ (Fig. 36a), large grains are observed. An epitaxial growth of the grains is visible in HAZ nearer to the fusion boundary (Fig. 36b) and a fine equiaxial crystal zone is visible in the HAZ (Fig. 36c) [58].

The Nd-YAG Laser welded part of Ti–50.9 at.% Ni with Ti–50.0 at.% Ni is shown in Fig. 37 [30]. The (a), (b) and (c) sides shown in the figure represents the

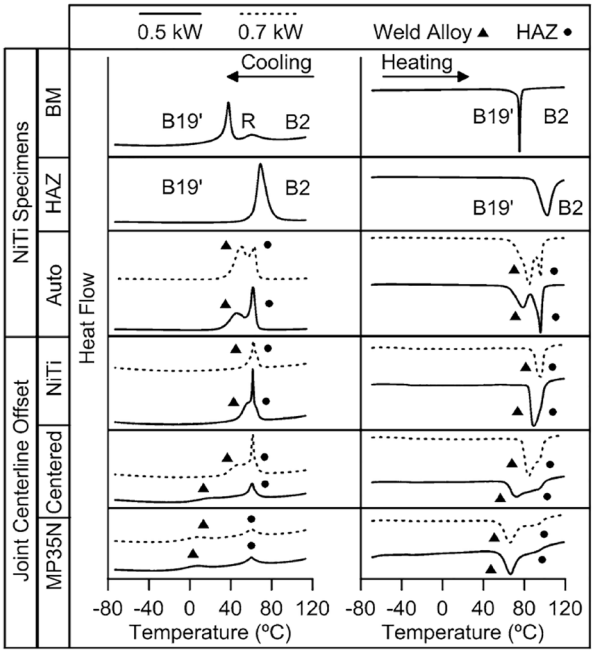

Fig. 34 DSC result by Panton et al. [60]

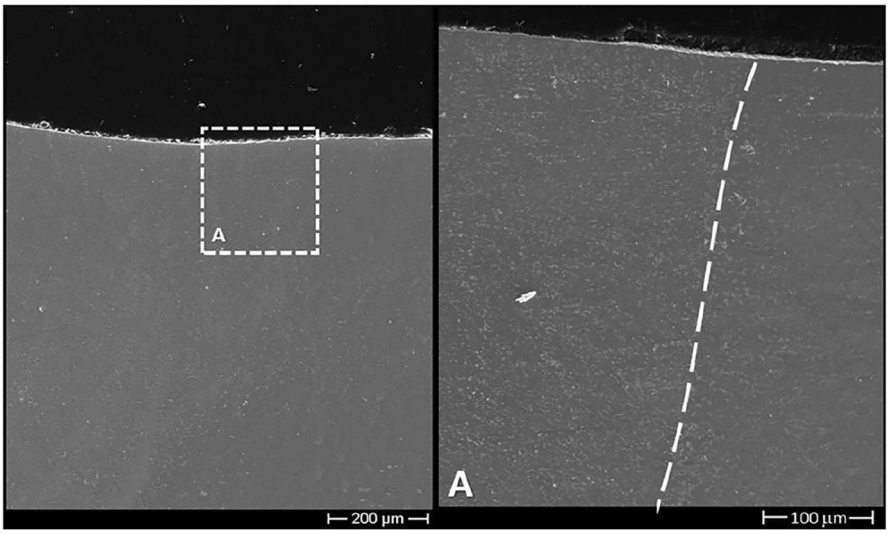

Fig. 35 SEM image of melting zone of laser welded NiTi and NiTiCu [69]

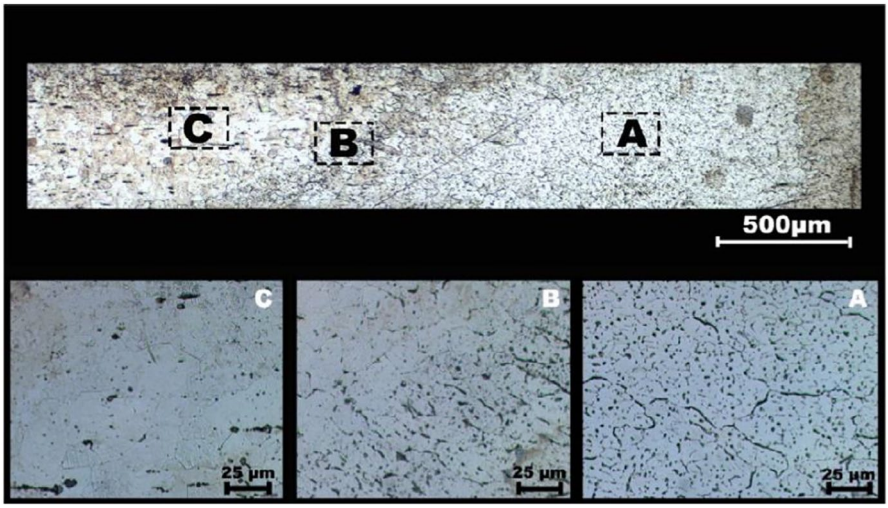

Fig. 36 Optical micrograph of cross-sectional view of NiTi-NiTiCu weld (**a**) FZ, (**b**) HAZ/ FZ, (**c**) HAZ [58]

base alloy with 50.9 at.%Ni, welded joint and base alloy with 50.0 at.% Ni. Little excessive penetration of the welded joint (b) is observed along with the side (c) of the weld have been attained in comparison to the opposite side [30].

Shamsolhodaei et al. [54] showed SEM and EBSD (Electron Back-Scattering Diffraction) IPF (Inverse Pole Figure) micrographs for the welded samples of both

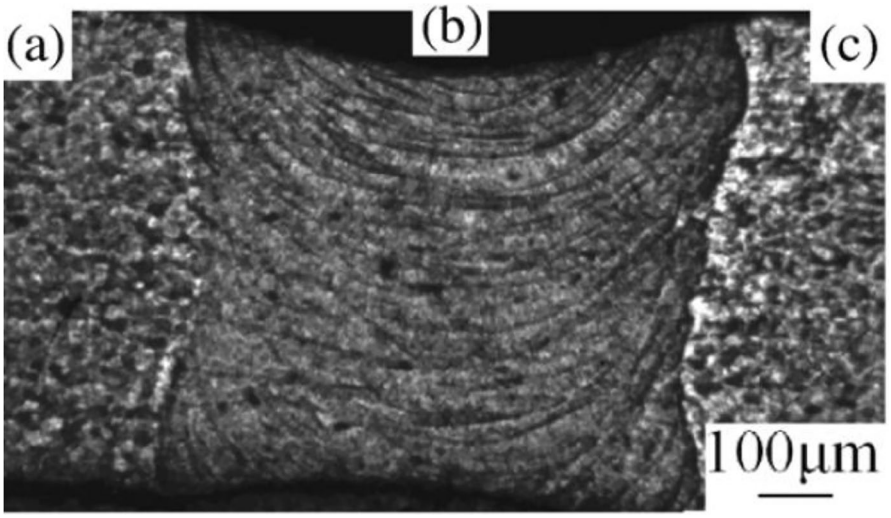

Fig. 37 Optical micrograph of the (**a**) HAZ of Ti–50.9 at.%Ni, (**b**) FZ and (**c**) HAZ of Ti–50.0 at.%Ni [30]

low and high laser power (Fig. 38). The formation of the unindexed regions is attributed to the evaporation of Ni while welding with a high-power (HP) laser. They have also noticed a change in plane direction from (111) to (100) for HP welding. The grain growth during the welding is observed by the Electron Probe Micro Analyzer (EPMA) as shown in Fig. 38b and d for LP and HP welded samples, respectively. The HP welded samples observed to have lower amount of Ni, as indicated by the blue colour in the region of FZ. This leads to formation of martensite phase in HP samples.

Gao et al. [70] welded a 50.2 at.% NiTi sheet with 301SS sheet using a fibre laser with a layer of pure Nb and Cu foil in between them (Fig. 39a). After welding, two layers are formed namely, NiTi-Nb interface (Layer I) and Nb-Cu-SS interface (Layer II). The optical image of the welded part is presented in the

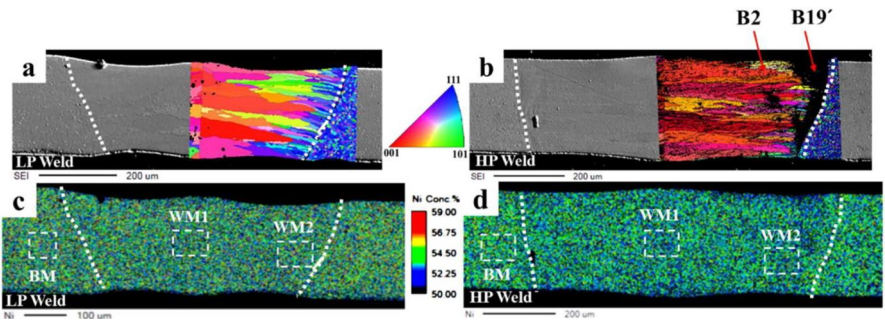

Fig. 38 (**a**, **c**) SEM micrograph and EBSD map for low high laser power weld samples and (**b**, **d**) EPMA map for low and high laser power weld samples [54]

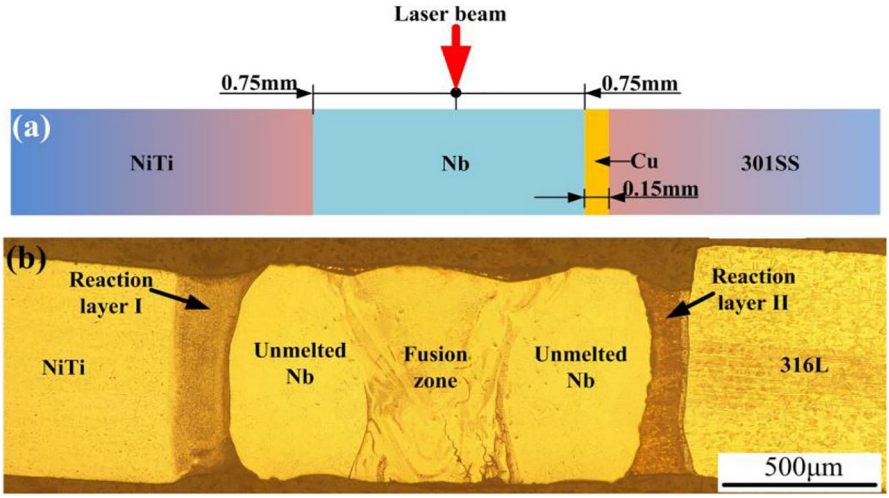

Fig. 39 (**a**) Schematic representation of the welding operation, (**b**) optical micrograph showing different zones after welding process [70]

Fig. 39b. These two different zones are formed because of high thermal conductivity of the Nb and Cu. When the HZ is created the heat produced in the melting pool is conducted towards the mentioned zones. When this heat exceeds the melting temperature of the interfaces, the layers are formed. In particular, the layer-I is formed when the temperature of the interface is more than 1170℃ (eutectic temperature of NiTi-Nb). Whereas in layer-II Cu is first melted and form a liquid phase in the Nb-Cu-SS interface. This liquid phase wets the Fe and Nb present in the zone which later diffuses into the liquid phase in small amount, which is confirmed by the XRD analysis of both layers (Fig. 40). A good crystal interface of NiTi-Nb is evident in Fig. 41a.

The TEM images of the NiTiNb and Ti6Al4V alloys welding is provided in Fig. 42. From Fig. 42a, it is observed that the microstructure is more columnar in nature in comparison to that noticed in Fig. 42b. The selected area electron diffraction (SAED) of the sections c and d suggests that the dendrite is primarily in a solid BCC state and the NiTi is in simple cubic structure (Fig. 42c and d).

Optimization Methods

The summary of the current review concerned with the similar and dissimilar welding of NiTi SMAs using the literature acquired by implementing the proposed SLR methodology is provided in Table 1. However, the study of SMA is still an incipient area for researchers and various industries and numerous efforts have been put forward every now and then in this domain due to its considerable utility. In the present scenario, major work that has been done on the joining of NiTi SMA is related to structural analysis and characterization of the properties of the joints. This leaves a

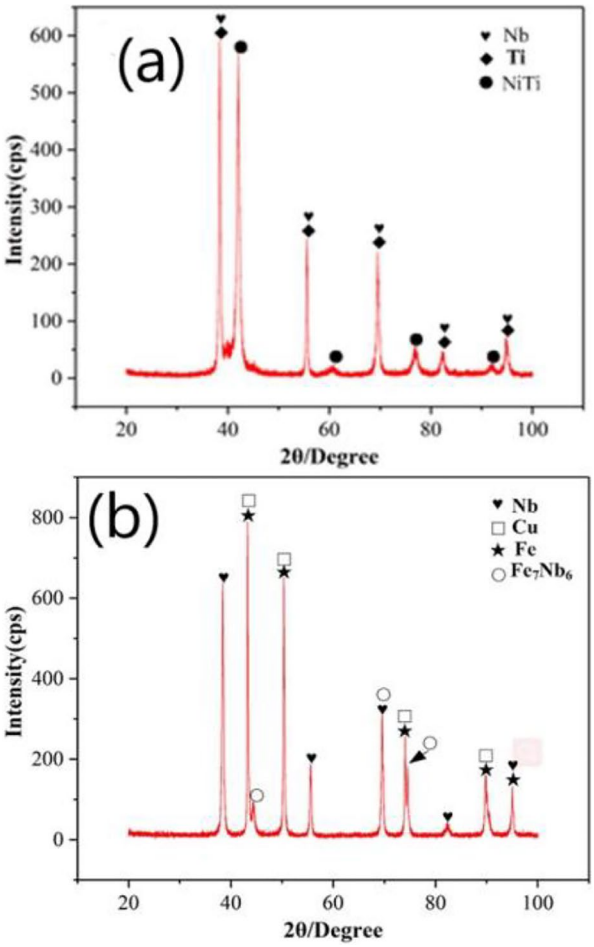

Fig. 40 XRD result of (**a**) NiTi-Nb Interface and (**b**) Nb-Cu-SS interface [70]

window open to another part of the study that is controlling the process parameters during joining/welding. By controlling the parameter combinations, it is possible to eliminate unwanted process combinations which do not affect the result significantly. For this purpose, optimization of process parameters is essential. During the literature survey, we noted that not much work on optimization for machining of NiTi SMA has been done. But the amount of paper on optimization of process parameters for Joining of NiTi SMA is comparatively lower. Few state-of-the-art studies related to optimization methods used during handling NiTi alloy are reviewed.

To reduce the time and cost, the experimentation is planned as per standardized (full factorial, Taguchi's L_9 [1, 38, 46] and L_{27} [11], L_{36} [78] and L_{65} [79] orthogonal array, response surface methodology (RSM) [80]) design of experiment (DOE) and the significant controllable parameters are identified. As proposed by previous researchers, the imperative process parameters for the Laser welding process are laser power, welding time, focal position and laser mode [11]. Otibar et al. [81]

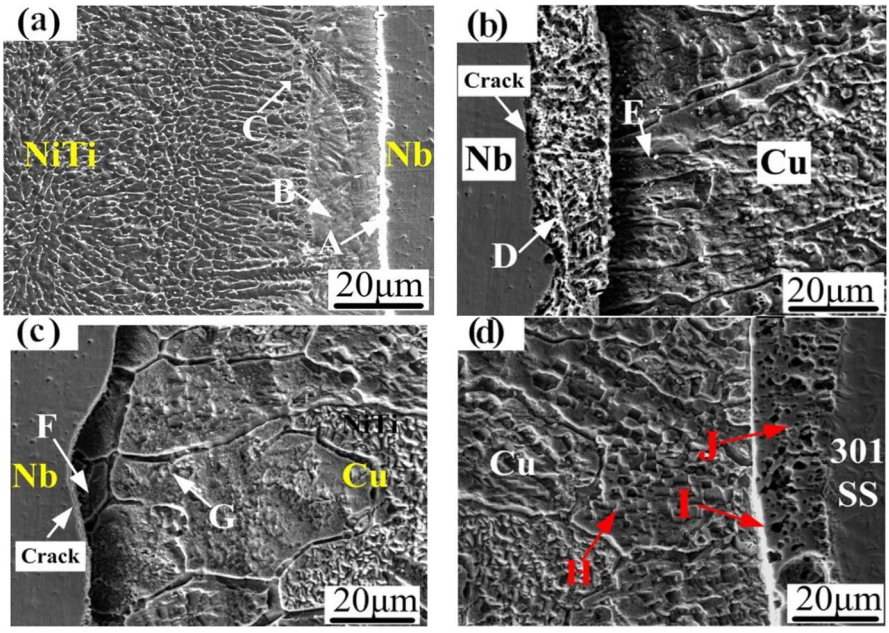

Fig. 41 SEM micrograph at the interface of (**a**) NiTi-Nb, (**b**) upper part of Nb-Cu, (**c**) lower part of Nb-Cu and (**d**) Cu-SS [70]

used a fractional full factorial DOE and carried out the laser welding of NiTi-NiTi. Other machining processes such as electric discharge machining (EDM) [78, 81, 82], wire EDM (WEDM) [80], electrochemical machining (ECM) [83] are explored for machining of NiTi SMA using optimization methods. Kanan et al. [72] used the Artificial Neural Network (ANN) method of optimization for the process parameters of laser welding of NiTi sheets. Neural power professional V2.5 software is used for this purpose. For multi-objective optimization researchers have adopted grey relational analysis(GRA) [67, 79, 84, 85], combined optimization using RSM and heat transfer search algorithm [38], RSM, multi-objective genetic algorithm(MOGA-II) [79] and Adaptive Particle Swarm Optimization (APSO) [86]. Therefore, it is understood that accompanying the need for investigation pertaining to the physical, mechanical, and metallurgical aspects of NiTi joining both in similar and dissimilar combination, there exists an adequate opportunity for the optimisation of desired responses via existing as well as modified techniques.

Conclusion

Owing to its industrial relevance and the complex and unique properties associated with NiTi alloy, the joining of these alloys need to be studied continuously and precisely. Among the available welding techniques, the Laser welding process is commonly used owing to its narrow HAZ, high power density, low distortion of

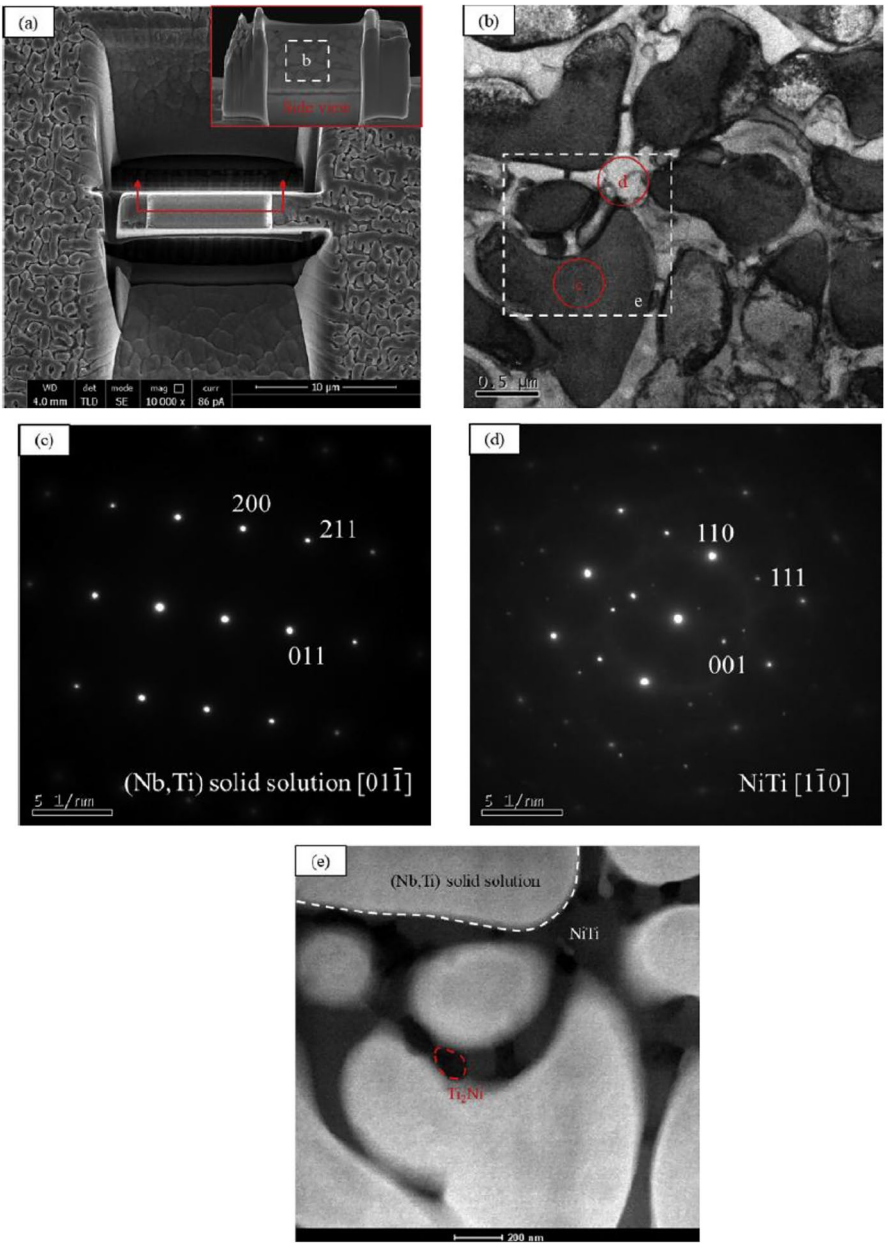

Fig. 42 TEM image of the dissimilar joining of NiTiNb and Ti6Al4V alloys [71]

the workpiece, no requirement of vacuum and relatively high quality of weld structure. In this systematic literature review, the challenges and progress on welding of NiTi SMAs in similar and dissimilar combinations are reported by highlighting

Table 1 Summary of the present SLR

Joining operation	Material type	Joining material	NiTi composition	Dimension	Author
TIG Welding	Wires and Sheets	NiTi-NiTi	Ti-55.3 wt% Ni	D = 0.75 mm t = 0.2 mm, w = 8 mm	Ikai et al. (1996) [19]
Laser welding	Wires	NiTi-NiTi	50.65 at.% Ni-49.10 at.%Ti	D = 100 µm	Gugel et al. (2008) [18]
Laser welding	Wires	NiTi-NiTi	Ti–50.0 at.%Ni and Ti–50.9 at.%Ni	D = 1 mm	Song et al. (2008) [30]
Friction Welding	Wires	NiTi-SS with Ni interlayer		D = 2.5 mm	Fukumoto et al. (2010) [43]
Laser welding	Wires	NiTi-NiTi	Ti-55.8 wt% Ni	D = 0.41 mm	Tam et al. (2011) [24]
Laser welding	Foil	NiTi-NiTi	Ti-55.91 wt% Ni	t = 0.25 mm	Chan et al. (2011) [31]
Laser welding	Wires	NiTi-SS with Ni interlayer	Ti–49.8 at.%Ni	t = 0.48 mm	Li et al. (2012) [48]
TIG welding	Tubes	NiTi-SS		Outer D = 9.53 mm NiTi inner D = 5.72 mm Cu wire D = 6.22 mm	Fox et al. (2012) [42]
Laser welding	Foil	NiTi-SS	56.4 wt%Ni–Ti	NiTi, t = 0.34 mm SS, t = 0.47 mm	Pouquet et al. (2012) [49]
Laser welding	Wires	NiTi-NiTi NiTi-SS	55 wt%Ni-45 wt%Ti	D = 0.36 mm	Mirshekari et al. (2013) [23]
Laser welding	Wires	NiTi-NiTi	Ti-55.91 wt% Ni	D = 0.5 mm	Chan et al. (2013) [64]
TIG Welding	Sheets	NiTi-NiTi	50.8 at.% Ni–Ti	t = 1.5 mm	Oliveira et al. (2016) [20]
Laser welding	Plates	NiTi- Ti_6Al_4V with Niobium interlayer	50.8 at.% Ni-49.25 at.% Ti	(30 × 30) mm	Oliveira et al. (2016) [50]
TIG welding	Wires	NiTi-TiMo		D = 0.5 mm	Costa et al. (2016) [41]
Laser welding	Sheet	NiTi-SS with Cu interlayer	Ni – 50.7 at.% Ti	t = 1 mm	Zoeram et al. (2017) [32]
Laser welding	NiTi wire Cu sheet	NiTi-Cu	50.8 at.% Ni–Ti	D = 700 µm t = 0.5 mm	Zeng et al. (2017) [39]
Laser welding	Sheets	NiTi-NiTi	55.64 wt%Ni-44.36 wt.% Ti	t = 1 mm	Kannan et al. (2017) [72]

Table 1 (continued)

Joining operation	Material type	Joining material	NiTi composition	Dimension	Author
Laser welding	Wires	NiTi-NiTi	Ti–55.8 wt.% Ni		Dong et al. (2018) [28]
Laser welding	Wires	NiTi-NiTi	Ti–55.8 wt.% Ni	D = 254 µm	Dong et al. (2018) [18]
Laser welding	Sheet	NiTi-NiTi	52 at.% Ni-48 at.% Ti	t = 1 mm	Datta et al. (2019) [27]
Laser welding	Wires	NiTi-NiTi	Ti-50.8 at% Ni	D = 250 µm	Yao et al. (2019) [17]
Laser welding	Wires	NiTi-316L SS	55.63 wt.% NiTi	D = 1 mm	Zhang et al. (2022) [73]
Nd:YAG Pulsed Laser welding	Wires	NiTi-NiTi	Ni(50.8 at.%)Ti	D = 380 µm	Shamsolhodaei et al. [52]
Fibre laser welding	Sheets	NiTi-301SS	Ni(50.2 at.%)Ti	t = 0.8 mm	Gao et al. [54]
Femtosecond Laser welding	Coupons	NiTi-NiTi	–	t = 0.4 mm	Quintino et al. [55]
Nd:YAG Pulsed Laser welding	Wires	NiTi-SS	50.2 at.% NiTi	t = 400 µm	Shamsolhodaei et al. [56]
Nd:YAG Pulsed Laser welding	Strip	NiTi-NiTi	55.8 wt.% NiTi	t = 0.37 mm	Michael et al. [57]
Femtosecond Laser welding	Wires	NiTi-NiTi	–	–	Quintino et al. [58]
Pulsed Nd:YAG laser	Wire	NiTi-NiTi	Ni (50.8 at.%) Ti	D = 700 µm	Michael et al. [59]
Pulsed Nd:YAG laser	Wire	NiTi-MP35N	–	D = 380 µm	Panton et al. [60]
YAG laser	Sheets	NiTi-Ti_2AlNb	Ni (51.9 at.%)Ti	t = 0.7 mm	Ge et al. [74]
Pulsed Nd:YAG laser	Wires	NiTi-Cu17Al11Mn	50.8 at.% NiTi	D = 0.5 mm	Oliveira et al. [75]
Nd:YAG laser welding	Sheet	NiTi-AISI304SS	Ti-49.4 at.% Ni	t = 0.2 mm	Wang et al. [51]
Continuous fiber laser	Wires	NiTi-316LSS	55.63 wt.% NiTi	D = 1 mm	Zhang et al. [73]
Pulsed Nd:YAG laser	Wires	NiTi-Cu	50.2 at.% NiTi	D = 400 µm	Shamsolhodaei et al. [34]
Nd:YAG laser	Wires	NiTi-AISI304SS	NiTi (45 at.%)	–	Asadi et al. [76]
Pulsed Nd:YAG laser	Sheets	NiTi-Ti_6Al_4V	Ni (47 at.%) Ti (44 at.%) Nb(9 at.%)	t = 300 µm	Zhou et al. [62]
Pulsed Nd:YAG laser	Wires	NiTi-NiTi	–	D = 0.38 mm	Panton et al. [63]

Table 1 (continued)

Joining operation	Material type	Joining material	NiTi composition	Dimension	Author
Nd:YAG laser	Sheet	NiTi-AISI304	Ti-49.4 at.% Ni	t = 0.2 mm	Chen et al. [38]
Nd:YAG laser	Wires	NiTi-NiTi	50.8 at.% NiTi	–	Shamsolhodaei et al. [65]
Nd:YAG laser	Sheets	NiTiNb	Ni47Ti44Nb9	t = 0.3 mm	Yuhua et al. [44]
Pulsed Nd:YAG laser	Tube	NiTi-NiTi	50.2 at.% NiTi	Inner D = 400 µm Outer D = 600 µm	Shamsolhodaei et al. [77]
Pulsed Nd:YAG laser	Plates	NiTi-Ti_6Al_4V	50.8 at. % NiTi	t = 1 ± 0.05 mm	Oliveira et al. [50]
Fiber laser	Wires	NiTi-304SS	Ni (55 wt.%) Ti	D = 1 mm	Zhang et al. [66]
Friction stir welding	Sheets	NiTi-Ti_6Al_4V	55.66 wt.% NiTi	t = 3 mm	Deng et al. [36]
Pulsed Laser Welding	Sheets	NiTiNb-Ti_6Al_4V	$Ni_{47}Ti_{44}Nb_9$	t = 0.2 mm	Zhong et al. [46]
Ultrasonic spot-welding	Sheets	NiTi-Ti_6Al_4V	55.66 wt.% NiTi	t = 0.25 mm	Xie et al. [35]

the mechanical, microstructural, and metallurgical aspects of the WZ and different methods of optimization of process parameters.

The currently implemented SLR methodology has significant advantages over the conventional literature review in the sense that, it momentously evaluates research articles with less time and more precision. However, it is worthy to mention that the criteria defined for the exclusion or inclusion of articles should be suitably selected as this is the key factor in deciding the effectiveness of this method. According to the SLR performed we note that, though numerous research is ongoing in this contemporary domain, welding of NiTi SMAs in a similar combination is more in comparison to the dissimilar combination. Also, the influence of application of fluxes alongside suitable edge preparation (as practised in conventional welding) of the plate/sheet/wire is yet to be reported during the joining of NiTi SMAs in similar/dissimilar conditions. Moreover, the assessment of economic efficiency with simultaneous environmental and societal benefit of the pursuance of laser spot welding technique for the joining of smart materials from sustainability perspective has not been performed so far. Therefore, more research work needs to be accomplished in this domain for better understanding and subsequent applicability. The number of research works using NiTi alloy wire is quite low as compared to NiTi sheet and/or plate. Though, using intermetallic layer have posed certain advantages, welding of NiTi SMAs using diverse intermetallic layer is limited and needs to be explored more. Very few numbers of studies are available on the optimization of process parameters for the laser welding of NiTi SMAs that leaves a window open for further research.

Data Availability Statement The authors declare that the data supporting the findings of this study are available within the article.

Declarations

Conflict of Interest The authors declare that they have no conflict of interest.

References

1. DeepanBharathiKannan, T., Sathiya, P., Ramesh, T.: Experimental investigation and characterization of laser welded NiTinol shape memory alloys. J. Manuf. Processes **25**, 253–261 (2017). https://doi.org/10.1016/j.jmapro.2016.12.006
2. Shayanfard, P., et al.: Stress raisers and fracture in shape memory alloys: review and ongoing challenges. Crit. Rev. Solid State Mater. Sci. **0**(0), 1–59 (2021). https://doi.org/10.1080/10408436.2021.1896475
3. Kramár, T., Tauer, J., Vondrous, P.: Welding of nitinol by selected technologies. Acta Polytech. **59**, 42–50 (2019). https://doi.org/10.14311/AP.2019.59.0042
4. Mehrpouya, M., Gisario, A., Lavvafi, H., Dehghanghadikolaei, A., Darafsheh, A.: Chapter 8 - Laser welding of nickel-titanium (NiTi) shape memory alloys. In: Paulo Davim, J., Gupta, K., Gupta, K., Paulo Davim, J. (eds.) Advanced Welding and Deforming, pp. 203–230. Elsevier (2021). https://doi.org/10.1016/B978-0-12-822049-8.00008-6

5. Mehrpouya, M., Gisario, A., Barletta, M., Natali, S., Veniali, F.: Dissimilar laser welding of NiTi wires. Lasers Manuf. Mater. Process. **6**(2), 99–112 (2019). https://doi.org/10.1007/s40516-019-00084-0
6. Lee, J., Shin, Y.C.: Effects of composition and post heat treatment on shape memory characteristics and mechanical properties for laser direct deposited nitinol. Lasers Manuf. Mater. Process. **6**(1), 41–58 (2019). https://doi.org/10.1007/s40516-019-0079-5
7. Shamsolhodaei, A., Oliveira, J.P., Panton, B., Ballesteros, B., Schell, N., Zhou, Y.N.: Superelasticity preservation in dissimilar joint of NiTi shape memory alloy to biomedical PtIr. Materialia **16**, 101090 (2021). https://doi.org/10.1016/j.mtla.2021.101090
8. Mehrpouya, M., Shahedin, A.M., Daood Salman Dawood, S., Kamal Ariffin, A.: An investigation on the optimum machinability of NiTi based shape memory alloy. Mater. Manuf. Processes **32**(13), 1497–1504 (2017). https://doi.org/10.1080/10426914.2017.1279290
9. Shehab, A.A., et al.: Laser welding of titanium grade 2 and aluminium AA 3105-O using a New AlSiCZr filler metal. Lasers Manuf. Mater. Process. (2022). https://doi.org/10.1007/s40516-021-00159-x
10. Mehrpouya, M., Gisario, A., Huang, H., Rahimzadeh, A., Elahinia, M.: Numerical study for prediction of optimum operational parameters in laser welding of NiTi alloy. Opt. Laser Technol. **118**, 159–169 (2019). https://doi.org/10.1016/j.optlastec.2019.05.010
11. Chan, C.-W., Man, H.C., Yue, T.: Parameter optimization for laser welding of NiTi wires by the Taguchi method. Lasers Eng. **30**, 247–265 (2015)
12. Pattanayak, S., Panda, S.: Laser beam micro drilling – a review. Lasers Manuf. Mater. Process. **5**(4), 366–394 (2018). https://doi.org/10.1007/s40516-018-0072-4
13. Thorpe, R., Holt, R.: The SAGE dictionary of qualitative management research. SAGE (2007)
14. Mengist, W., Soromessa, T., Legese, G.: Method for conducting systematic literature review and meta-analysis for environmental science research. MethodsX **7**, 100777 (2020). https://doi.org/10.1016/j.mex.2019.100777
15. Siksnelyte-Butkiene, I.: A systematic literature review of indices for energy poverty assessment: a household perspective. Sustainability **13**(19), 19 (2021). https://doi.org/10.3390/su131910900
16. Wang, Y. et al.: Numerical simulation of ultrasonic spot welding of superelastic NiTi alloys: temperature distribution and deformation behavior. J. Manuf. Sci. Eng. **144**(8) (2022). https://doi.org/10.1115/1.4053523
17. Yao, R., Dong, P., Liaw, P.K., Zhou, J., Wang, W.: Microstructure and shape memory effect of laser welded Nitinol wires. Mater. Lett. **238**, 1–5 (2019). https://doi.org/10.1016/j.matlet.2018.11.141
18. Dong, P., Li, H., Wang, W., Zhou, J.: Microstructural characterization of laser micro-welded Nitinol wires. Mater. Charact. **135** (2017). https://doi.org/10.1016/j.matchar.2017.11.022
19. Ikai, A., Kimura, K., Tobushi, H.: TIG welding and shape memory effect of TiNi shape memory alloy. J. Intell. Mater. Syst. Struct. **7**(6), 646–655 (1996). https://doi.org/10.1177/1045389X9600700604
20. Oliveira, J.P., Barbosa, D., BrazFernandes, F., Miranda, R.M.: Tungsten inert gas (TIG) welding of Ni-rich NiTi plates: Functional behavior. Smart Mater. Struct. **25**, 03LT01 (2016). https://doi.org/10.1088/0964-1726/25/3/03LT01
21. Quazi, M.M., et al.: A comprehensive assessment of laser welding of biomedical devices and implant materials: recent research, development and applications. Crit. Rev. Solid State Mater. Sci. **46**(2), 109–151 (2021). https://doi.org/10.1080/10408436.2019.1708701
22. Oliveira, J.P., Miranda, R.M., BrazFernandes, F.M.: Welding and joining of NiTi shape memory alloys: a review. Progress Mater. Sci. **88**, 412–466 (2017). https://doi.org/10.1016/j.pmatsci.2017.04.008
23. Mirshekari, G.R., Saatchi, A., Kermanpur, A., Sadrnezhaad, S.K.: Laser welding of NiTi shape memory alloy: Comparison of the similar and dissimilar joints to AISI 304 stainless steel. Opt. Laser Technol. **54**, 151–158 (2013). https://doi.org/10.1016/j.optlastec.2013.05.014
24. Tam, B., Khan, M.I., Zhou, Y.: Mechanical and Functional Properties of Laser-Welded Ti-55.8 Wt Pct Ni Nitinol Wires. Metall. Mater. Trans. A **42**(8), 2166–2175 (2011). https://doi.org/10.1007/s11661-011-0639-6
25. Naffakh-Moosavy, H., Rasouli, A.: Similar Joining of NiTi Shape Memory Alloy using Nd:YAG Pulsed Laser Welding. J Welding Sci. Technol. Iran **7**(2), 89–101 (2022)
26. Gugel, H., Schuermann, A., Theisen, W.: Laser welding of NiTi wires. Mater. Sci. Eng., A **481–482**, 668–671 (2008). https://doi.org/10.1016/j.msea.2006.11.179

27. Datta, S., Raza, M.S., Saha, P., Pratihar, D.K.: Effects of process parameters on the quality aspects of weld-bead in laser welding of NiTinol sheets. Mater. Manuf. Processes **34**(6), 648–659 (2019). https://doi.org/10.1080/10426914.2019.1566608
28. Dong, P., et al.: Microstructure and corrosion resistance of laser-welded crossed nitinol wires. Materials (Basel) **11**(5), E842 (2018). https://doi.org/10.3390/ma11050842
29. Chan, C.W., Man, H.C.: Reduction of environmentally induced cracking of laser-welded shape memory NiTi wires via post-weld heat-treatment. Mater. Sci. Eng., A **588**, 388–394 (2013). https://doi.org/10.1016/j.msea.2013.09.051
30. Song, Y.G., Li, W.S., Li, L., Zheng, Y.F.: The influence of laser welding parameters on the microstructure and mechanical property of the as-jointed NiTi alloy wires. Mater. Lett. **62**(15), 2325–2328 (2008). https://doi.org/10.1016/j.matlet.2007.11.082
31. Chan, C.W., Man, H.C., Yue, T.M.: Effects of process parameters upon the shape memory and pseudo-elastic behaviors of laser-welded NiTi thin foil. Metall. Mater. Trans. A **42**(8), 2264–2270 (2011). https://doi.org/10.1007/s11661-011-0623-1
32. ShojaeiZoeram, A., Rahmani, A., Akbari Mousavi, S.A.A.: Microstructure and properties analysis of laser-welded Ni–Ti and 316l sheets using copper interlayer". J. Manuf. Processes **26**, 355–363 (2017). https://doi.org/10.1016/j.jmapro.2017.02.005
33. Sun, Q., et al.: Study on weld formation and segregation mechanism for dissimilar pulse laser welding of NiTi and Cu wires. Opt. Laser Technol. **140**, 107071 (2021). https://doi.org/10.1016/j.optlastec.2021.107071
34. Shamsolhodaei, A., Sun, Q., Wang, X., Panton, B., Di, H., Zhou, Y.N.: Effect of Laser Positioning on the Microstructure and Properties of NiTi-Copper Dissimilar Laser Welds. J. Mater. Eng. Perform **29**(2), 849–857 (2020). https://doi.org/10.1007/s11665-020-04637-9
35. Xie, J., Chen, Y., Yin, L., Zhang, T., Wang, S., Wang, L.: Microstructure and mechanical properties of ultrasonic spot welding TiNi/Ti6Al4V dissimilar materials using pure Al coating. J. Manuf. Process **64**, 473–480 (2021). https://doi.org/10.1016/j.jmapro.2021.02.009
36. Deng, H., et al.: Microstructure and mechanical properties of dissimilar NiTi/Ti6Al4V joints via back-heating assisted friction stir welding. J. Manuf. Process. **64**, 379–391 (2021). https://doi.org/10.1016/j.jmapro.2021.01.024
37. Rodrigues, L.F.A., Amorim, F.A., Grassi, E.N.D., dos Santos, P.L.L., de Araújo, C.J.: TIG spot welding applied to NiTi shape memory wires optimized by factorial design. Int. J. Adv. Manuf. Technol. **121**(11), 7749–7762 (2022). https://doi.org/10.1007/s00170-022-09848-z
38. Chen, Y., Sun, S., Zhang, T., Zhou, X., Li, S.: Effects of post-weld heat treatment on the microstructure and mechanical properties of laser-welded NiTi/304SS joint with Ni filler. Mater. Sci. Eng., A **771**, 138545 (2020). https://doi.org/10.1016/j.msea.2019.138545
39. Zeng, Z., Oliveira, J.P., Yang, M., Song, D., Peng, B.: Functional fatigue behavior of NiTi-Cu dissimilar laser welds. Mater. Des. **114**, 282–287 (2017). https://doi.org/10.1016/j.matdes.2016.11.023
40. Huang, G.Q., Yan, Y.F., Wu, J., Shen, Y.F., Gerlich, A.P.: Microstructure and mechanical properties of fine-grained aluminum matrix composite reinforced with nitinol shape memory alloy particulates produced by underwater friction stir processing. J. Alloy. Compd. **786**, 257–271 (2019). https://doi.org/10.1016/j.jallcom.2019.01.364
41. Costa, J.D., et al.: Obtaining and characterization of Ni-Ti/Ti-Mo joints welded by TIG process. Vacuum **133**, 58–69 (2016). https://doi.org/10.1016/J.VACUUM.2016.08.016
42. Fox, G., Hahnlen, R., Dapino, M.J.: Fusion welding of nickel–titanium and 304 stainless steel tubes: Part II: tungsten inert gas welding. J. Intell. Mater. Syst. Struct. **24**(8), 962–972 (2013). https://doi.org/10.1177/1045389X12461076
43. Fukumoto, S., Inoue, T., Mizuno, S., Okita, K., Tomita, T., Yamamoto, A.: Friction welding of TiNi alloy to stainless steel using Ni interlayer. Sci. Technol. Weld. Joining **15**(2), 124–130 (2010). https://doi.org/10.1179/136217109X12577814486692
44. Yuhua, C., Yuqing, M., Weiwei, L., Peng, H.: Investigation of welding crack in micro laser welded NiTiNb shape memory alloy and Ti6Al4V alloy dissimilar metals joints. Opt. Laser Technol. **91**, 197–202 (2017). https://doi.org/10.1016/j.optlastec.2016.12.028
45. Cheng, Q., Guo, N., Zhang, D., Fu, Y., Zhang, S., He, J.: Study on interface and mechanical property of laser welding of NiTi shape memory alloy and 2A12 aluminum alloy joint with a TC4 wire. Smart Mater. Struct. **31**(1), 015032 (2021). https://doi.org/10.1088/1361-665X/ac3d71
46. Zhong, Y., Xie, J., Chen, Y., Yin, L., He, P., Lu, W.: Microstructure and mechanical properties of micro laser welding NiTiNb/Ti6Al4V dissimilar alloys lap joints with nickel interlayer. Mater. Lett. **306**, 130896 (2022). https://doi.org/10.1016/j.matlet.2021.130896

47. Teshome, F.B., et al.: Microstructure, macrosegregation, and mechanical properties of NiTi to Ti6Al4V dissimilar laser welds using Co interlayer. J. Mater. Eng. Perform (2022). https://doi.org/10.1007/s11665-022-07064-0
48. Li, H.M., Sun, D.Q., Cai, X.L., Dong, P., Wang, W.Q.: Laser welding of TiNi shape memory alloy and stainless steel using Ni interlayer. Mater. Des. **39**, 285–293 (2012). https://doi.org/10.1016/j.matdes.2012.02.031
49. Pouquet, J., Miranda, R.M., Quintino, L., Williams, S.: Dissimilar laser welding of NiTi to stainless steel. Int. J. Adv. Manuf. Technol. **61** (2011). https://doi.org/10.1007/s00170-011-3694-7
50. Oliveira, J.P., et al.: Laser joining of NiTi to Ti6Al4V using a Niobium interlayer. Acta Mater. **105**, 9–15 (2016). https://doi.org/10.1016/j.actamat.2015.12.021
51. Wang, H., Xie, J., Chen, Y., Liu, W., Zhong, W.: Effect of CoCrFeNiMn high entropy alloy interlayer on microstructure and mechanical properties of laser-welded NiTi/304 SS joint. J. Market. Res. **18**, 1028–1037 (2022). https://doi.org/10.1016/j.jmrt.2022.03.022
52. Mehrpouya, M., Gisario, A., Broggiato, G.B., Puopolo, M., Vesco, S., Barletta, M.: Effect of welding parameters on functionality of dissimilar laser-welded NiTi superelastic (SE) to shape memory effect (SME) wires. Int. J. Adv. Manuf. Technol. **103**(1), 1593–1601 (2019). https://doi.org/10.1007/s00170-019-03514-7
53. Krishnakumari, A., Saravanan, M., Sarvesh, J.: Application of Nd: YAG laser in Nano WC surface alloying with low carbon austenitic steel in predicting the microstructure and hardness. Lasers Manuf. Mater. Process. **8**(2), 201–215 (2021). https://doi.org/10.1007/s40516-021-00145-3
54. Shamsolhodaei, A., Razmpoosh, M.H., Maletta, C., Magaro, P., Zhou, Y.N.: A comprehensive insight into the superelasticity measurement of laser welded NiTi shape memory alloys. Mater. Lett. **287**, 129310 (2021). https://doi.org/10.1016/j.matlet.2021.129310
55. Ge, F., et al.: Dissimilar laser welding of a NiTi shape memory alloy to Ti2AlNb. Metals **11**(10), 10 (2021). https://doi.org/10.3390/met11101578
56. Shamsolhodaei, A., Oliveira, J.P., Schell, N., Maawad, E., Panton, B., Zhou, Y.N.: Controlling intermetallic compounds formation during laser welding of NiTi to 316L stainless steel. Intermetallics **116**, 106656 (2020). https://doi.org/10.1016/j.intermet.2019.106656
57. Oliveira, J.P., et al.: Dissimilar laser welding of superelastic NiTi and CuAlMn shape memory alloys. Mater. Des. **128**, 166–175 (2017). https://doi.org/10.1016/j.matdes.2017.05.011
58. Mehrpouya, M., Gisario, A., Brotzu, A., Natali, S.: Laser welding of NiTi shape memory sheets using a diode laser. Opt. Laser Technol. **108**, 142–149 (2018). https://doi.org/10.1016/j.optlastec.2018.06.038
59. Mehrpouya, M., Gisario, A., Barletta, M., Broggiato, G.B.: Welding strength of dissimilar laser-welded NiTi and NiTiCu shape memory wires. Manuf. Lett. **22**, 25–27 (2019). https://doi.org/10.1016/j.mfglet.2019.10.003
60. Panton, B., Pequegnat, A., Zhou, Y.N.: Dissimilar laser joining of NiTi SMA and MP35N wires. Metall. Mater. Trans. A. **45**(8), 3533–3544 (2014)
61. Li, J., Panton, B., Mao, Y., Vivek, A., Daehn, G.: High-strength micro impact welding of NiTi wire to brass sheet. Weld World **66**(9), 1799–1809 (2022). https://doi.org/10.1007/s40194-022-01336-y
62. Asadi, S., Saeid, T., Valanezhad, A., Watanabe, I., Khalil-Allafi, J.: Effects of Ni powder addition on microstructure and mechanical properties of NiTi to AISI 304 stainless steel archwire dissimilar laser welds. J. Manuf. Process. **55**, 13–21 (2020). https://doi.org/10.1016/j.jmapro.2020.03.041
63. Michael, A., Pequegnat, A., Wang, J., Zhou, Y.N., Khan, M.I.: Corrosion performance of medical grade NiTi after laser processing. Surf. Coat. Technol. **324**, 478–485 (2017). https://doi.org/10.1016/j.surfcoat.2017.05.092
64. Chan, C.W., Man, H.C., Yue, T.M.: Effect of post-weld heat-treatment on the oxide film and corrosion behaviour of laser-welded shape memory NiTi wires. Corros. Sci. **56**, 158–167 (2012). https://doi.org/10.1016/j.corsci.2011.11.020
65. Mirshekari, G.R., Kermanpur, A., Saatchi, A., Sadrnezhaad, S.K., Soleymani, A.P.: Microstructure, cyclic deformation and corrosion behavior of laser welded NiTi shape memory wires. J. Mater. Eng. Perform **24**(9), 3356–3364 (2015). https://doi.org/10.1007/s11665-015-1614-y
66. Mandal, M., Patra, S., Chakraborty, R., Saha, P., Shome, M.: Microstructural evolution and nanoindentation study of magnetic pulse welded Nitinol and Aluminium sheets. Mater. Charact. **184**, 111690 (2022). https://doi.org/10.1016/j.matchar.2021.111690

67. Pequegnat, A., Michael, A., Wang, J., Lian, K., Zhou, Y., Khan, M.I.: Surface characterizations of laser modified biomedical grade NiTi shape memory alloys. Mater. Sci. Eng. C **50**, 367–378 (2015). https://doi.org/10.1016/j.msec.2015.01.085
68. Michael, A., Zhou, Y.N., Yavuz, M., Khan, M.I.: Deconvolution of overlapping peaks from differential scanning calorimetry analysis for multi-phase NiTi alloys. Thermochim. Acta **665**, 53–59 (2018). https://doi.org/10.1016/j.tca.2018.05.014
69. Mehrpouya, M., Gisario, A., Barletta, M., Veniali, F.: Investigation on the functionality of laser-welded NiTi to NiTiCu shape memory wires. J. Intell. Mater. Syst. Struct. **31**(9), 1171–1175 (2020). https://doi.org/10.1177/1045389X20914401
70. Gao, X.-L., Wang, X.-Q., Liu, J., Li, L.: A novel laser welding method for the reliable joining of NiTi/301SS. Mater. Lett. **268**, 127573 (2020)
71. Zhou, X., Chen, Y., Huang, Y., Mao, Y., Yu, Y.: Effects of niobium addition on the microstructure and mechanical properties of laser-welded joints of NiTiNb and Ti6Al4V alloys. J. Alloy. Compd. **735**, 2616–2624 (2018). https://doi.org/10.1016/j.jallcom.2017.11.307
72. Kannan, T.D.B., Ramesh, T., Sathiya, P.: Application of Artificial Neural Network Modelling for Optimization of Yb: YAG Laser Welding of Nitinol. Trans. Indian Inst. Met. **70**(7), 1763–1771 (2017). https://doi.org/10.1007/s12666-016-0973-x
73. Zhang, K., Liu, F., Tan, C., Zhou, Y.N., Peng, P.: Effect of heat input modes on microstructure, mechanical properties and porosity of laser welded NiTi-316L joints: A comparative study. Mater. Sci. Eng. A **848**, 143426 (2022). https://doi.org/10.1016/j.msea.2022.143426
74. Tam, B., Pequegnat, A., Khan, M.I., Zhou, Y.: Resistance microwelding of Ti-55.8 wt pct Ni nitinol wires and the effects of pseudoelasticity. Metall. Mater. Trans. A **43**(8), 2969–2978 (2012). https://doi.org/10.1007/s11661-012-1115-7
75. Zhang, K., Peng, P., Zhou, Y.N.: Laser welding-brazing of NiTi/304 stainless steel wires with beam defocus and large offset. Mater. Sci. Eng. A **835**, 142660 (2022). https://doi.org/10.1016/j.msea.2022.142660
76. Shamsolhodaei, A., Zhou, Y.N., Michael, A.: Enhancement of mechanical and functional properties of welded NiTi by controlling nickel vapourisation. Sci. Technol. Weld. Joining **24**(8), 706–712 (2019). https://doi.org/10.1080/13621718.2019.1595926
77. Tuissi, A., Besseghini, S., Ranucci, T., Squatrito, F., Pozzi, M.: Effect of Nd-YAG laser welding on the functional properties of the Ni–49.6at.%Ti. Mater. Sci. Eng. A **273–275**, 813–817 (1999). https://doi.org/10.1016/S0921-5093(99)00422-0
78. Gaikwad, V., Jatti, V.S.: Optimization of material removal rate during electrical discharge machining of cryo-treated NiTi alloys using Taguchi's method. J. King Saud Univ. Eng. Sci. **30**(3), 266–272 (2018). https://doi.org/10.1016/j.jksues.2016.04.003
79. Mohammed, M.K., Al-Ahmari, A.: Laser-machining of microchannels in NiTi-based shape-memory alloys: experimental analysis and process optimization. Materials **13**(13), 13 (2020). https://doi.org/10.3390/ma13132945
80. Chaudhari, R., Vora, J.J., Prabu, S.S.M., Palani, I.A., Patel, V.K., Parikh, D.M.: Pareto optimization of WEDM process parameters for machining a NiTi shape memory alloy using a combined approach of RSM and heat transfer search algorithm. Adv. Manuf. **9**(1), 64–80 (2021). https://doi.org/10.1007/s40436-019-00267-0
81. Otibar, D., Rathmann, C., Lygin, K., Kreimeier, D., Szymansky, P.: Analyzing laser-welded NiTi-NiTi-joints for actuator applications using design of experiments. JMEA **5**(2) (2015). https://doi.org/10.17265/2159-5275/2015.02.003
82. Daneshmand, S., Kahrizi, E.F., LotfiNeyestanak, A.A., Monfared, V.: Optimization of electrical discharge machining parameters for Niti shape memory alloy by using the taguchi method. J. Mar. Sci. Technol. Taiwan **22**(4), 506–512 (2014). https://doi.org/10.6119/JMST-013-0624-1
83. Das, B., Parimanik, S.R., Mahapatra, T.R., Mishra, D.: Machinability assessment of NiTinol shape memory alloy in electrochemical machining. Int. J. Mach. Mach. Mater. **24**(3–4), 280–313 (2022). https://doi.org/10.1504/IJMMM.2022.125200
84. Sadeghi, A., Babakhani, A., Zebarjad, S.M., Mostajabodaveh, H.: Use of grey relational analysis for multi-objective optimisation of NiTiCu shape memory alloy produced by powder metallurgy process. J. Intell. Mater. Syst. Struct. **25**(16), 2093–2101 (2014). https://doi.org/10.1177/1045389X13517312
85. Parimanik, S.R., Mahapatra, T.R., Mishra, D., Rout, A.K.: Optimisation of performance characteristics in laser welding of Nitinol wires using Taguchi and grey relation analysis. Adv. Mater. Process. Technol. **0**(0), 1–10 (2022). https://doi.org/10.1080/2374068X.2022.2088653

86. Mishra, L., Mahapatra, T.R., Mishra, D., Pattanaik, S.K.: Machinability analysis and multiple performance optimization during laser micro-drilling of CNT reinforced polymer nanocomposite. Lasers Manuf. Mater. Process. **9**(2), 151–172 (2022). https://doi.org/10.1007/s40516-022-00171-9

Publisher's Note Springer Nature remains neutral with regard to jurisdictional claims in published maps and institutional affiliations.

Springer Nature or its licensor (e.g. a society or other partner) holds exclusive rights to this article under a publishing agreement with the author(s) or other rightsholder(s); author self-archiving of the accepted manuscript version of this article is solely governed by the terms of such publishing agreement and applicable law.